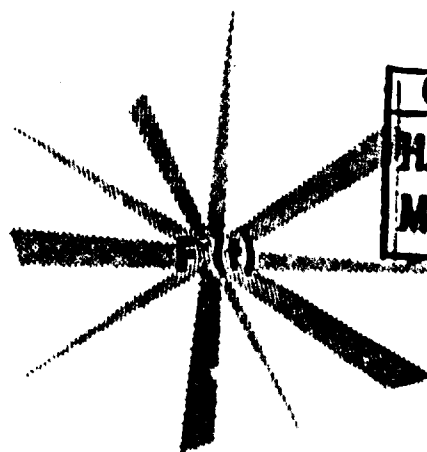


AD617544

AIR FORCE FLIGHT DYNAMICS LABORATORY

VEHICLE DYNAMICS DIVISION

SOD AND MATTED LANDING
SURFACE ROUGHNESS CHARACTERISTICS



COPY	OF	10
HARD COPY		\$ 3.00
MICROFICHE		\$ 0.75

54

AUTHOR
B. H. GROOMES

DDC
JUL 6 1965
TISA B

TECHNICAL MEMORANDUM NO.

FDDS-TM-64-32

DEC 1964

Best Available Copy

PROCESSING COPY

ARCHIVE COPY

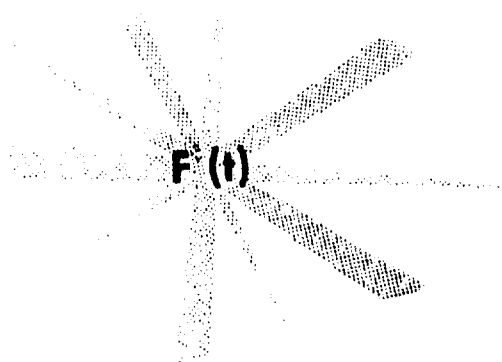
EVALUATION COPY

OK CPTT
see Dayton OH

AIR FORCE FLIGHT DYNAMICS LABORATORY

VEHICLE DYNAMICS DIVISION

**SOD AND MATTED LANDING
SURFACE ROUGHNESS CHARACTERISTICS**



AUTHOR

B. H. GROOMES

TECHNICAL MEMORANDUM NO.


FDDS-TM-64-32

FOREWORD

This report was prepared by the Aerospace Dynamics Branch, Vehicle Dynamics Division, Air Force Flight Dynamics Laboratory, Wright-Patterson Air Force Base, Ohio. The particular data presented were obtained in support of the F-5 System Program Office, Aeronautical Systems Division. This report is part of a continuing effort to provide rational and reliable dynamic load design criteria for flight vehicles and is part of the Research and Technology Division, Air Force Systems Command's exploratory development program. This effort is in support of Project 1370 "Dynamic Problems in Flight Vehicles", Task 137008 "Prediction and Prevention of Dynamic Load Problems". This report covers work conducted from August 1964 to September 1964.

The author expresses his appreciation to Messrs. Edmund Hotz and John Ach of the Field Measurements Group, Aerospace Dynamics Branch for their assistance in the data gathering phase; John Derrickson, Warren Smith, Ire Saxton and James Marable of the RTD digital computer programming and data converting facilities for their services and enthusiastic cooperation in the data reduction phase of the program. Additional appreciation is expressed to Major Maurice A. Reep, USMC, and the special Marine Corps group assigned to assist in gathering data at the United States Marine Corps matted field, Twenty-Nine Palms, California.

This report has been reviewed and is approved.


WELDON R. BAIRD, Major, USAF
Chief, Aerospace Dynamics Branch
Vehicle Dynamics Division

ABSTRACT

Limited sod and matted surface characteristics in the form of profile and power spectral density plots, discrete bump and dip distributions and maximum heights and depths for various wavelengths are presented. These runway roughness data were obtained from profile surveys of the Hughes Aircraft Company's sod field and the United States Marine Corps, Twenty-Nine Palms California multi-matted runway. The multi-matted runway was constructed from Convair aluminum matting (first 1500 feet), pierced steel planking (second 3500 feet) and M9M1 aluminum matting (last 1000 feet).

The power spectral densities for the sod and multi-matted surfaces show higher roughness characteristics than the power spectral density for the roughest prepared surface which had been previously established from a survey of 25 air bases throughout the United States. Also, for the limited data gathered, the multi-matted surface was rougher than the sod surface. When a comparison is made between the M9M1 and Convair aluminum matting and the pierced steel planking, it is apparent that the higher roughness characteristics of the multi-matting are due primarily to the pierced steel planking. Significant discrete and narrow band power peaks are evident in the power spectra of the matted surface over the reduced frequency (λ) range of approximately 6 radians per foot to .2 radian per foot which corresponds to wavelengths ranging from approximately one foot to thirty feet. To a lesser degree, peaks are also present in the power spectra of the sod field. However, the large discrete frequency components, which may be attributed to joints in the case of matted surface, are not present in the sod field data.

TABLE OF CONTENTS

SECTION		PAGE
I	Introduction	1
II	Equipment and Data Processing	2
III	Site Description	3
IV	Discussion of Results	4
V	Conclusions	7
VI	References	46

ILLUSTRATIONS

FIGURE	PAGE
1 Operation of Runway Profile Measuring Instrumentation .	8
2 Profiles, Hughes Sod Field	9
3 Four Feet by Four Feet Convair Aluminum Matting	10
4 M-6 Pierced Steel Planking	11
5 M9M1 Aluminum Matting	12
6 Profiles, Runway 31, USMC Base, Twenty-Nine Palms	13
7 Landing Surface Power Spectral Density Comparisons . .	14
8 Landing Surface Power Spectral Density, Hughes Sod Field	15
9 Landing Surface Power Spectral Density, Hughes Sod Field	16
10 Landing Surface Power Spectral Density, Hughes Sod Field	17
11 Hughes Sod Field PSD Comparisons (First Half of the Runway Compared to the Second Half)	18
12 Landing Surface Power Spectral Density, Runway 31, USMC Base, Twenty-Nine Palms.	19
13 Landing Surface Power Spectral Density, Runway 31, USMC Base, Twenty-Nine Palms.	20
14 Landing Surface Power Spectral Density, Runway 31, USMC Base, Twenty-Nine Palms.	21
15 Landing Surface Power Spectral Density, Runway 31, USMC Base, Twenty-Nine Palms.	22
16 Convair Aluminum Matting Profile.	23
17 Landing Surface Power Spectral Density, Runway 31, USMC Base, Twenty-Nine Palms.	24

ILLUSTRATIONS (Cont'd)

FIGURE		PAGE
18	Multi-Matted Runway PSD Comparisons (First Half of the Convair Matting Compared with the Last Half)	25
19	Multi-Matted Runway PSD Comparisons (First Half of the Pierced Steel Planking Compared with the Last Half). .	26
20	Multi-Matted Runway PSD Comparisons (First Half of the M9MI Aluminum Matting Compared with the Last Half) . .	27
21	Distribution of Maximum Bump Heights and Wavelengths (Hughes Sod Field)	28
22	Distribution of Maximum Dip Depths and Wavelengths (Hughes Sod Field)	29
23	Distribution of Maximum Bump Heights and Wavelengths (Multi-Matted Surface)	30
24	Distribution of Maximum Dip Depths and Wavelengths (Multi-Matted Surface)	31

LIST OF TABLES

TABLE		PAGE
1	Distribution of Bumps by Height and Wavelength (Hughes Sod Field)	32
2	Distribution of Dips by Depth and Wavelength (Hughes Sod Field)	36
3	Distribution of Bumps by Height and Wavelength (Multi-Matted Surface)	40
4	Distribution of Dips by Depth and Wavelength (Multi-Matted Surface)	43

SECTION I

INTRODUCTION

A requirement to extend the landing capabilities of certain current aircraft to include sod and semi-prepared surface operation, as well as a projection of this requirement to advanced vehicle concepts, has dictated a need for engineering data which define the roughness characteristics of these surfaces. These data are required to perform vehicle ground-induced dynamic loads analyses. This report presents the results of a limited investigation to provide these roughness characteristics for sod and multi-matted surfaces.

Runway roughness surveys of the Hughes Aircraft Company's sod field runway, Culver City, California and the United States Marine Corps' multi-matted surface runway, Twenty-Nine Palms, California, were performed at the request of the F-5 System Program Office (ASZJT), ASD, dated July 1964, in support of the F-5 Ground Loads Investigation Program. The surveys were accomplished from 17 to 22 August 1964 and the data were reduced from 26 August 1964 to 28 September 1964.

The surveys consisted of profile measurements of a sod area, which is located on the far side of the Hughes prepared surface runway (S W direction) and the USMC Base multi-matted surface runway 31, which consists of three types of matting as described in Section III.

The data reduction was accomplished by an AFFDL program previously established to provide surface profile and power spectral density (PSD) characteristics. This program is based on the equations in Reference 2 and is described in Section II.

SECTION II

EQUIPMENT AND DATA PROCESSING

The Automatic Profile Measuring Instrumentation of the Air Force Flight Dynamics Laboratory was used for these surveys. The equipment description has been documented in Reference 1. The description of a strip chart recorder is contained in Reference 2. The basic set-up and principle of operation of the equipment is shown in Figure 1. To prevent misalignment errors caused by equipment sinkage, plywood bearing pads were used under principal collimator bearing points (wheel and outriggers).

The data were reduced with a 7090 computer by the RTD digital computation group using a previously established program based on equations presented in Reference 2. Data reliability aspects have been considered for these types of data and included in the program. Power spectral densities were calculated from the profile data by the method described in Reference 2. This method incorporates the removal of a linear trend.

SECTION III

SITE DESCRIPTION

1. Sod Field

The sod field soil was adobe with a California Bearing Ratio (CBR) of 18 at the time of the survey. The field slopes twenty-eight feet in 9000 feet, and had been used for the F-5 vehicle landings, take-offs and taxi runs. The surface has ruts varying in depth from one inch to four inches and contains randomly occurring grass-patch bumps. Three lines of survey were made. One line of survey was made on the assumed centerline. Two additional lines of survey were then made each five feet six inches on the right and left hand side of the centerline. This corresponds to the lateral spacing of the F-5 main gear. The lines of survey were measured in a southwesterly direction. Figure 2 shows the surface shape and the lines of survey.

2. Multi-Matted Surface

The multi-matted field was a lake bed with a CBR of 27. A soil with a maximum density of 137 lbs/ft³ was used as a fill which provided an overall CBR of 25. The field slopes 150 feet in 1500 feet and has been used by cargo aircraft ranging from the C-47 to C-130 size for approximately two years. This particular field afforded an unusual opportunity for obtaining matted surface data, since the first 1500 feet was constructed from 4' x 4' Convair aluminum matting, the middle 3500 feet was constructed from M-6 pierced steel planking, and the last 1000 feet was constructed from M9M1 aluminum matting. The photographs shown in Figures 3, 4, and 5 illustrate the variations of the multi-matted field. Figure 6 shows the surface shape and the location of the three types of matting. Two lines of survey were made in the direction of runway 31. One line on the centerline included the three types of mats. The other line was made five feet six inches right side of center only on the steel planking surface.

SECTION IV

DISCUSSION OF RESULTS

1. Power Spectral Densities

The power spectral density (PSD) for the Hughes sod field (Figure 7) shows higher roughness characteristics at all reduced frequencies than the roughest prepared surface PSD presented in References 2 and 3. Increases in power by factors of approximately 3, 4, and 8 are evident and correspond to reduced frequency ranges of 0.01 to 0.1, 0.1 to 1, 1 to 2π radians per foot respectively. Corresponding wavelengths are 200π to 20π feet, 20π to 2π feet, and 2π feet to 1 foot respectively. Significant power peaks are evident in the medium and high reduced frequency range for specific spatial frequencies (Figures 7, 8, 9, and 10). A comparison of the PSD for the first half (southwest direction) of the runway contrasted with the PSD for the second half of the runway shows that the second half is rougher (Figure 11).

The multi-matted field PSD given in Figure 7 shows roughness characteristics that are higher than either the roughest prepared surface PSD or the sod field PSD for all reduced frequency ranges. Power increases by factors of 5, 10, and 15 are evident when the multi-matted surface PSD is compared to the roughest prepared surface PSD. Similarly, power increases by factors of 1.8, 3 and 8 can be seen when the multi-matted surface is compared to the sod surface PSD. These factors are within the reduced frequency ranges mentioned above. The panel spacings and deformations of the pierced steel planking were primarily responsible for the higher peaks in the power spectra (Figures 3, 4, 5, 7, 12, and 13). Significant peaks are evident at specific reduced frequencies associated with each type of matting. In the case of the pierced steel planking, there are two predominant peaks associated with the joint bumps which are approximately one and a quarter feet (5.03 rad/foot) and a multiple of this at wavelengths of two and one half feet (2.51 rad/foot). The power spectrum for this surface at five feet six inches on the right hand side of the center also shows these peaks (Figure 14). The power spectrum for the M9M1 aluminum matting shows three discrete peaks associated with the joints and multiples of the joint wavelengths (Figure 15). Figure 16 is a reproduction of a section of the profile plot of the Convair aluminum matting (4' x 4'). In the figure, square wave type profiles are presented with amplitudes varying from one-half inch to one inch. This square wave profile characteristic is apparently due to the joint and plank displacements occurring during vehicle loading (in this case the profile measuring instrumentation and towing vehicle). However, PSD peaks are not as predominant as was the case for the pierced steel planking and M9M1 matting. This is due to the peculiar nature of the wave shape and longer wavelengths that this type matting exhibited. At best, it can be seen that the power associated with this particular characteristic is represented by the slight upward curvature of the power

spectrum in Figure 17 at the critical reduced frequencies of approximately 1.2 to .3 for wavelengths ranging between five and twenty feet.

Aircraft landings and take-offs are made on runway 31 always in the same direction such that the Convair aluminum matting is encountered first, the pierced steel planking second and M9M1 aluminum matting last. Taxiing onto and off of the runway is accomplished at the pierced steel planking part of the runway. A comparison of the power spectra for the first (southeast) and last halves of the initial Convair matting (Figure 18) shows that the first half is considerably rougher probably due to landing impact from the various aircraft. A comparison of PSD's for the first and last half of the pierced steel planking (Figure 19) shows that the last half is rougher, possibly resulting from surface forming during braking action of the roll-out phases of aircraft operation. A comparison of PSD's for the first and last half of the M9M1 matting (Figure 20) shows very little difference in power levels with the last half containing slightly higher powers, particularly at the high reduced frequencies (short wave lengths). This may be associated with aircraft turning and other ground maneuvers prior to taxiing to the nearest taxi strip, which for this runway is located at the pierced steel planking portion of the runway.

2. Discrete Bump and Dip Distributions

Discrete bump and dip data were obtained for the centerline of each runway. These data were obtained from the measured profile characteristics which were plotted to a scale of one inch per ten feet of surface profile length and one inch per five inches of elevation. The bump or dip was determined from a straight line drawn through two points on the profile which provided a reasonable 1-cosine (bump) or cosine-1(dip) shape. The height or depth was measured normal to the line at or close to the midpoint of the wavelength where the nearest maximum peak occurred. Obvious bumps or dips were measured in a random manner, i.e., as the bumps or dips occurred. Thus random wavelengths were also obtained. The wavelengths were determined to an accuracy of ± 0.5 feet. The heights and depths were determined to an accuracy of ± 0.25 inches.

Tables 1, 2, 3, and 4 present the frequency of occurrence of various values of heights, depths and wavelengths respectively. Figures 21, 22, 23 and 24 present maximum heights and depths of the discrete bumps and dips respectively for various wavelengths.

Those bumps and dips obtained from the first half of each runway were compared with those obtained from the second half of the runway. In the case of the multi-matted runway, data from the three types of mats are reported separately.

The amplitudes of the bumps and dips obtained from the last or northwest half of the Hughes Sod Field were higher in magnitude for all wavelengths than those obtained from the first half. This agrees with the trend shown by the PSD data of Figure 11. The amplitudes of the bumps and dips were (1) greater on the first half of the Convair matting than the last half, (2) greater on the last half of the pierced steel planking than the first half, and (3) greater on the last half of the M9M1 matting than the first half for all wavelengths. This agrees with the trend previously discussed and shown by the power spectra in Figures 18, 19, and 20.

SECTION V

CONCLUSIONS

The power spectra for the sod and multi-matted surveys in this limited investigation show higher roughness than the power spectrum for roughest prepared surface which had been previously established from surveys of 25 air bases throughout the United States.

From the limited data gathered, the multi-matted surface was rougher than the sod surface.

The higher roughness characteristics of the multi-matting is due primarily to the pierced steel planking.

Significant power peaks are evident in the sod and matted surfaces. Discrete power peaks were particularly prominent at the wavelengths corresponding to the joints in the mats (or multiples of joint lengths) for the matted surfaces.

For the matted surface, there seems to be some correlation between the surface roughness and the type of aircraft operation (landing impact, braking, turn around, etc.) accomplished on particular section of the runway. For example, the landing impact area seemed to have increased roughness. Also areas where heavy braking usually occurs had higher roughness than sections farther down the runway, as discussed in preceding sections of the report. Both power spectra and discrete bump and dip data show the same trends in this correlation.

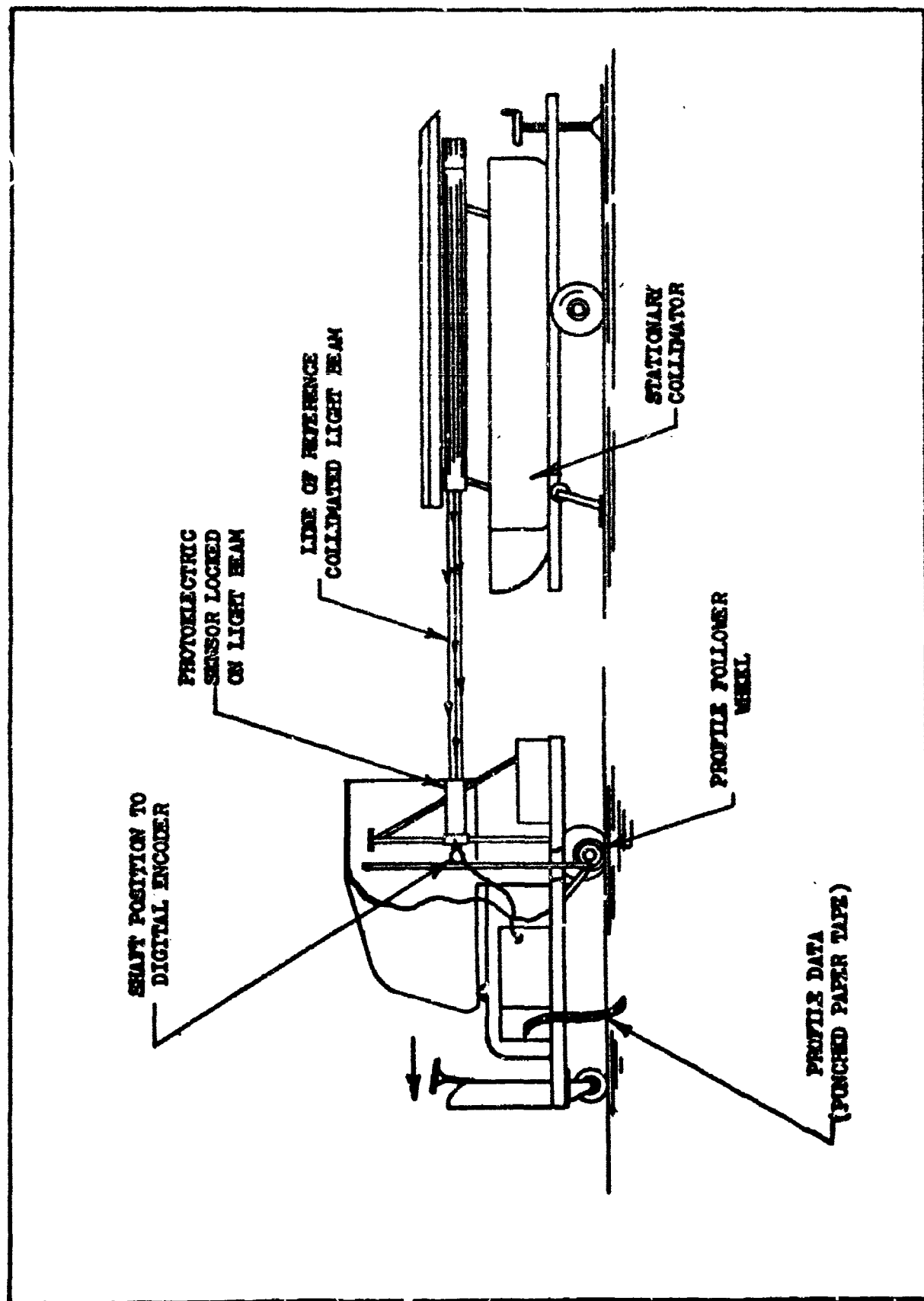
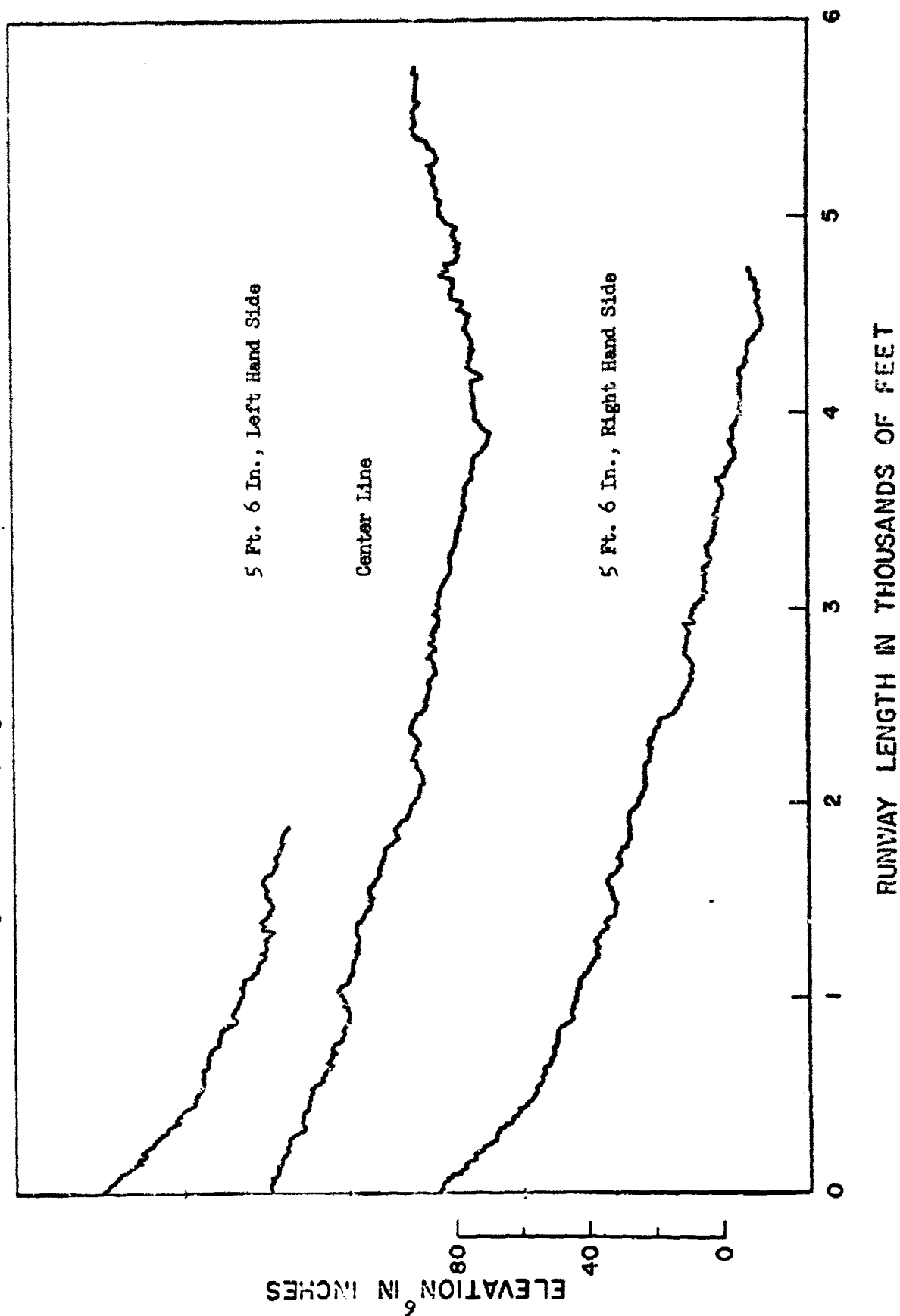


Fig. 1 Operation of Runway Profile Measuring Instrumentation

Fig. 2 Profile, Hughes Sod Field



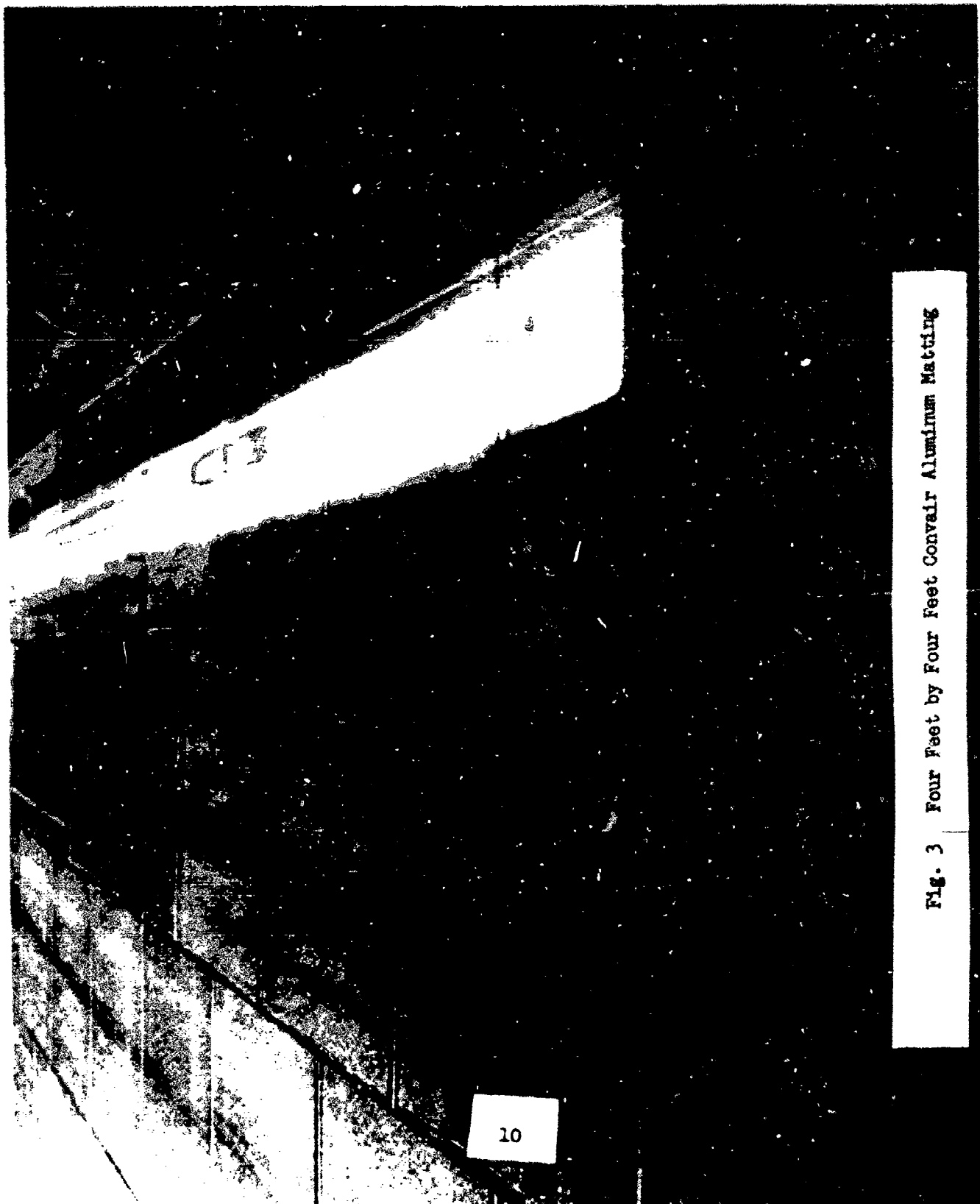
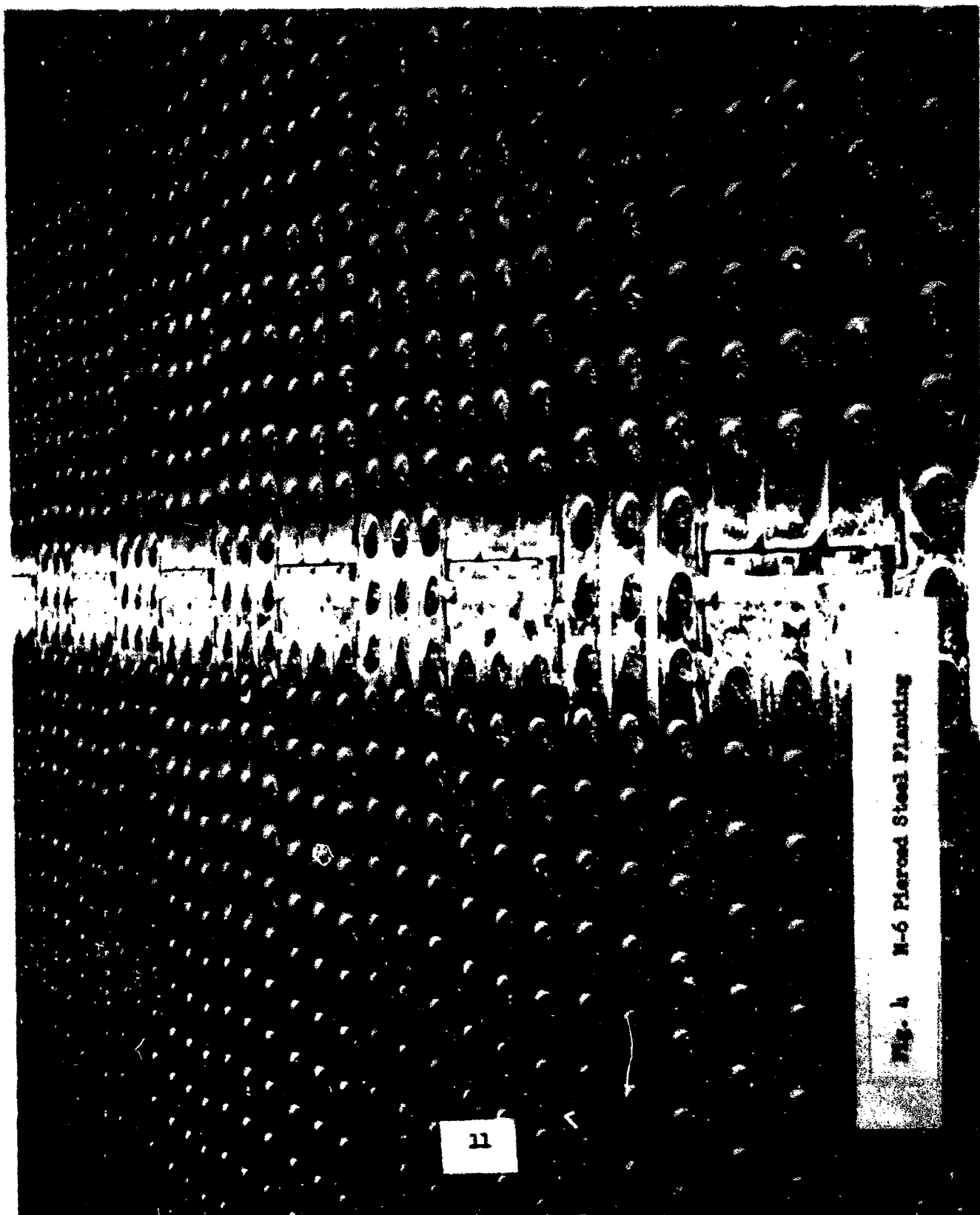


Fig. 3 Four Feet by Four Feet Convair Aluminum Matting



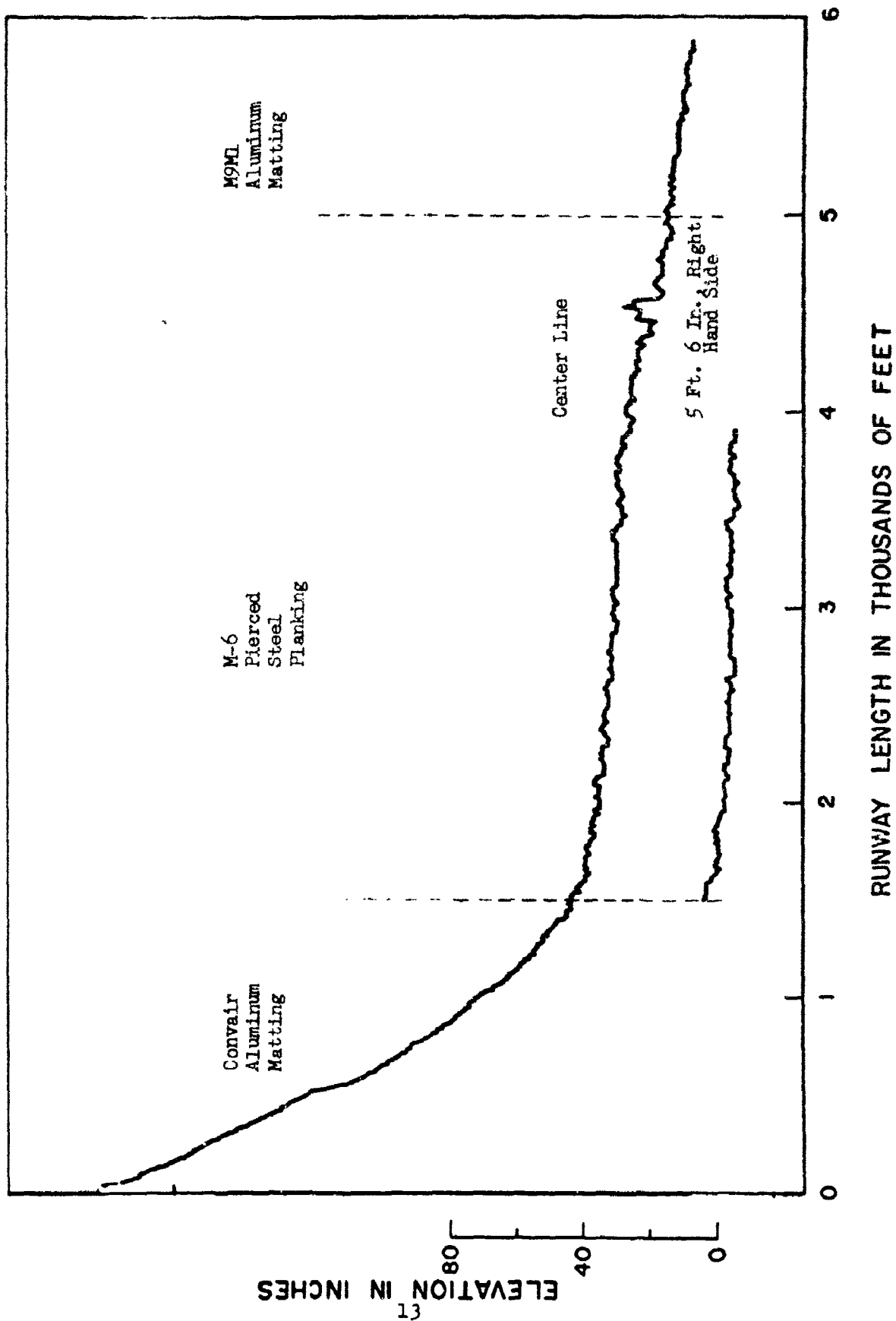
11

Fig. 4 N-6 Pierced Steel Planking



Fig. 5 M9M Aluminum Matting

Fig. 6 Profiles, Runway 31, USMC Base, Twenty-Nine Palms



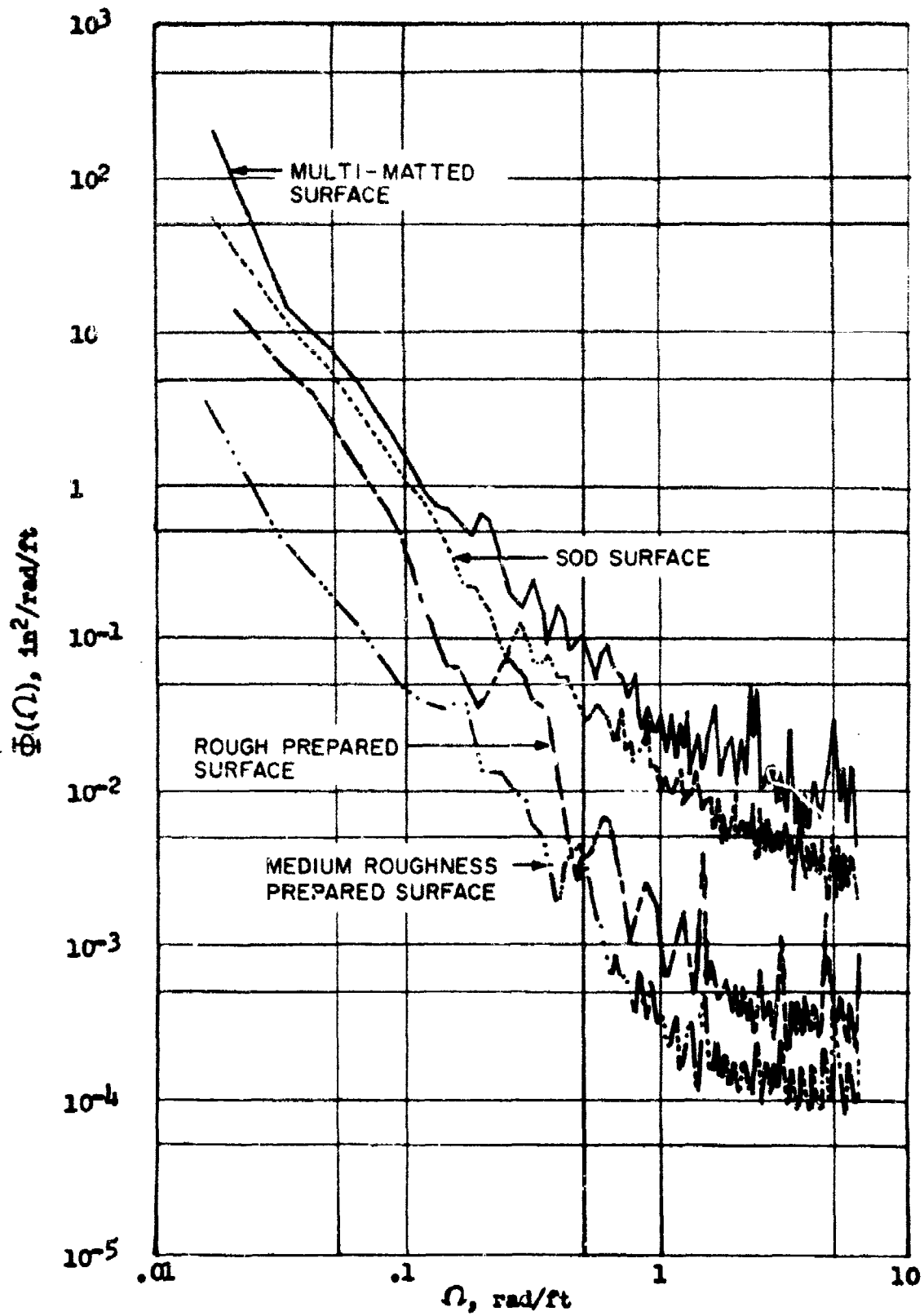


Fig. 7 Landing Surface Power Spectral Density Comparisons

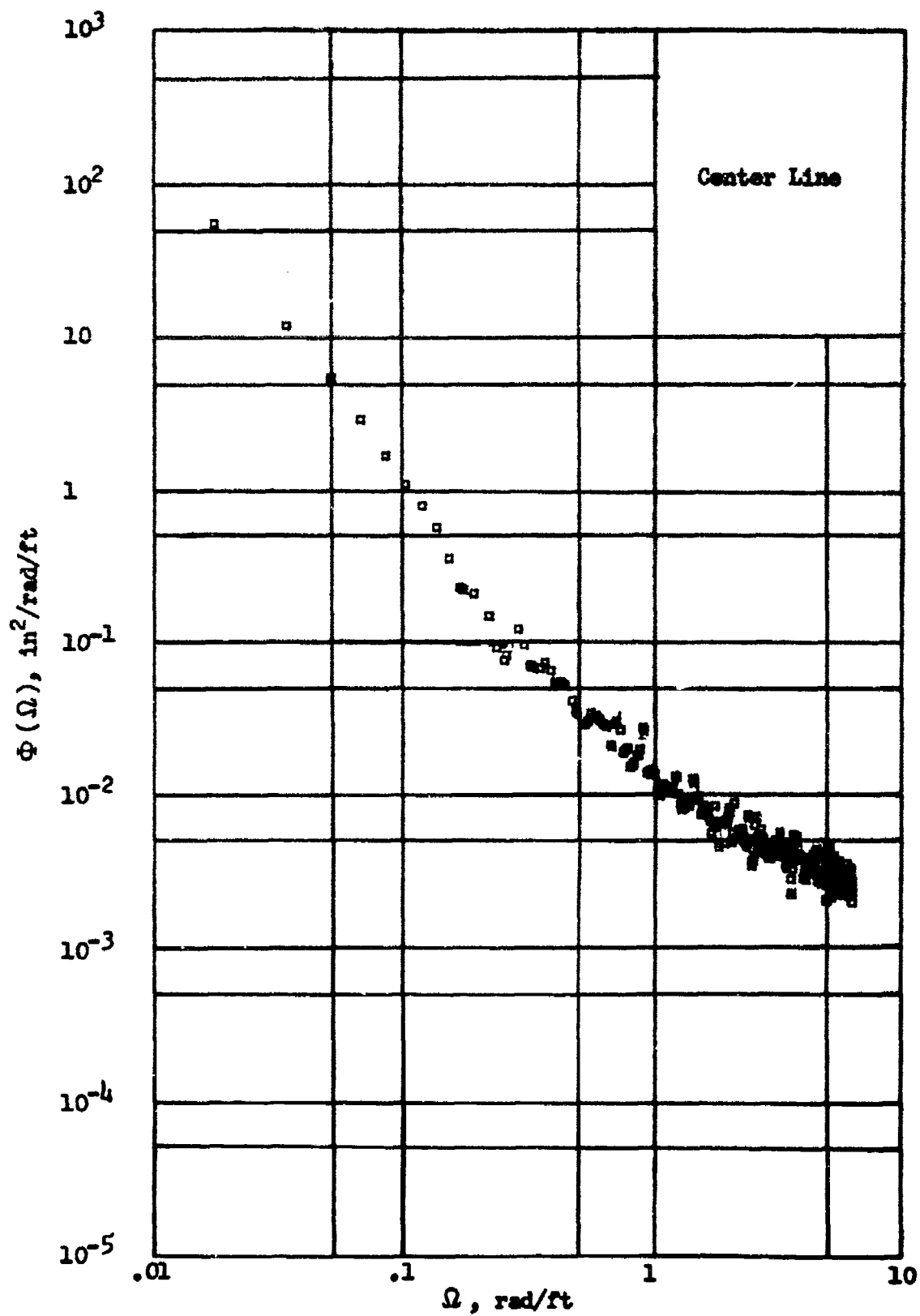


Fig. 8 Landing Surface Power Spectral Density, Hughes Sod Field

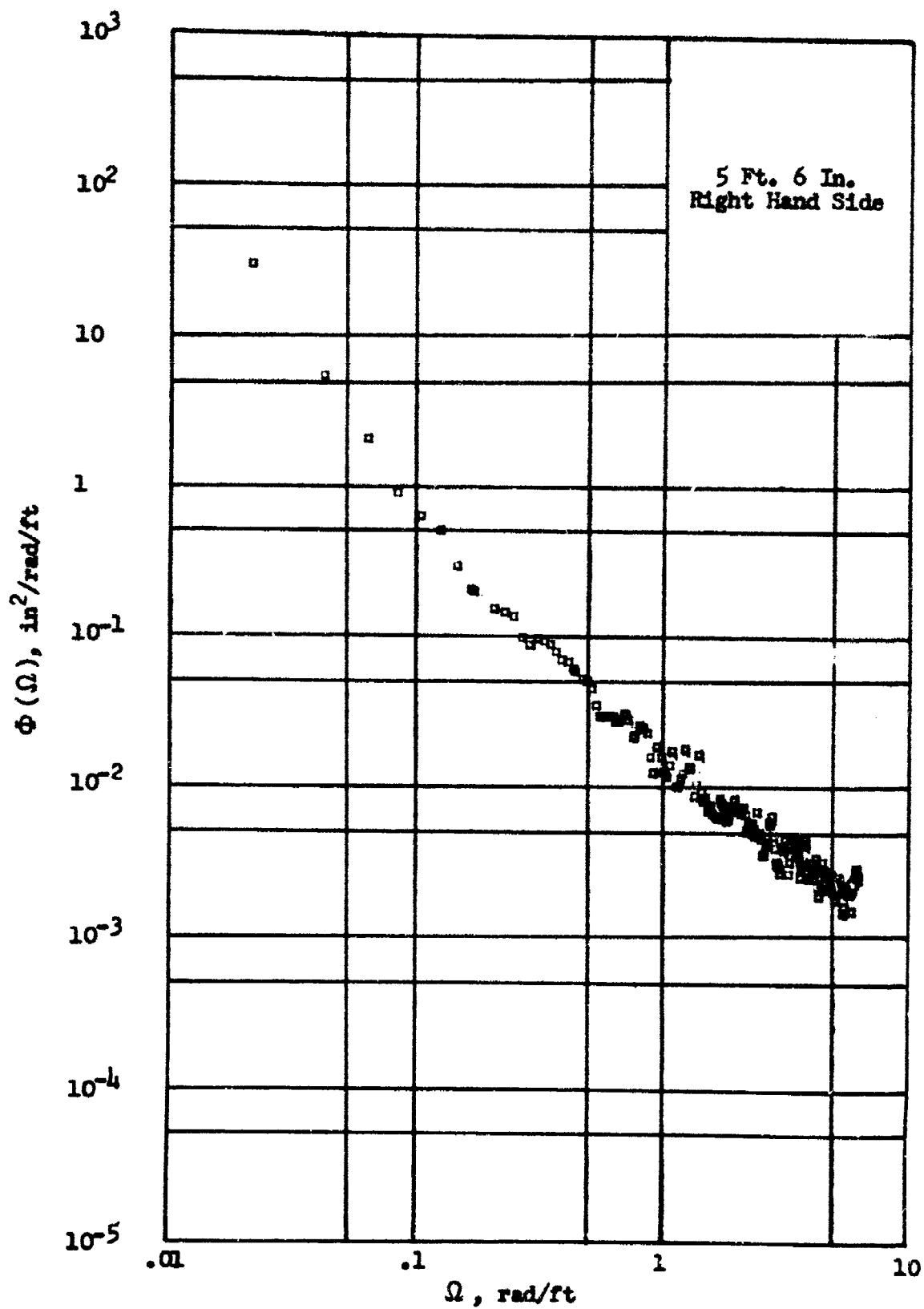


Fig. 9 Landing Surface Power Spectral Density, Hughes Sod Field

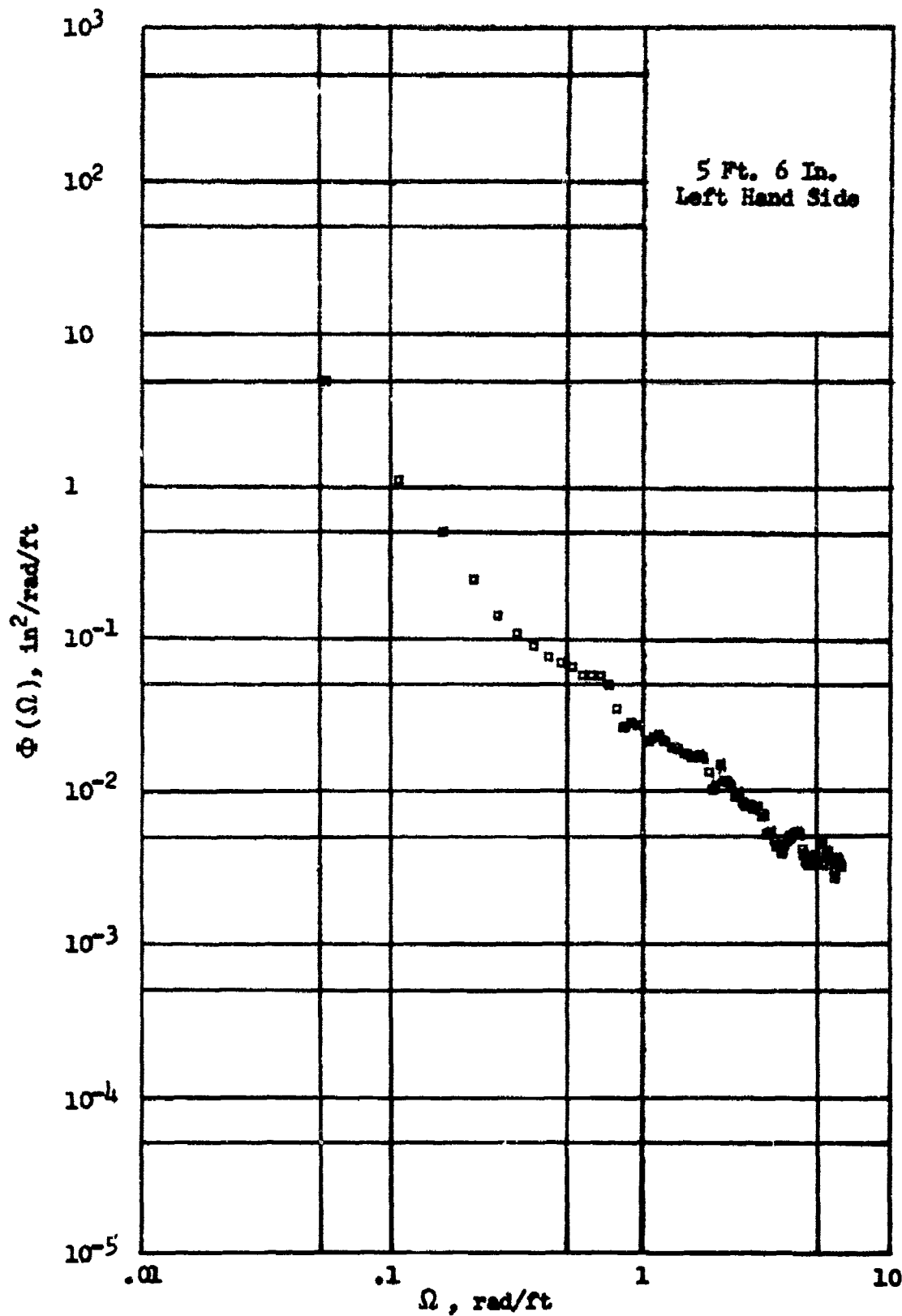


Fig. 10 Landing Surface Power Spectral Density, Hughes Sod Field

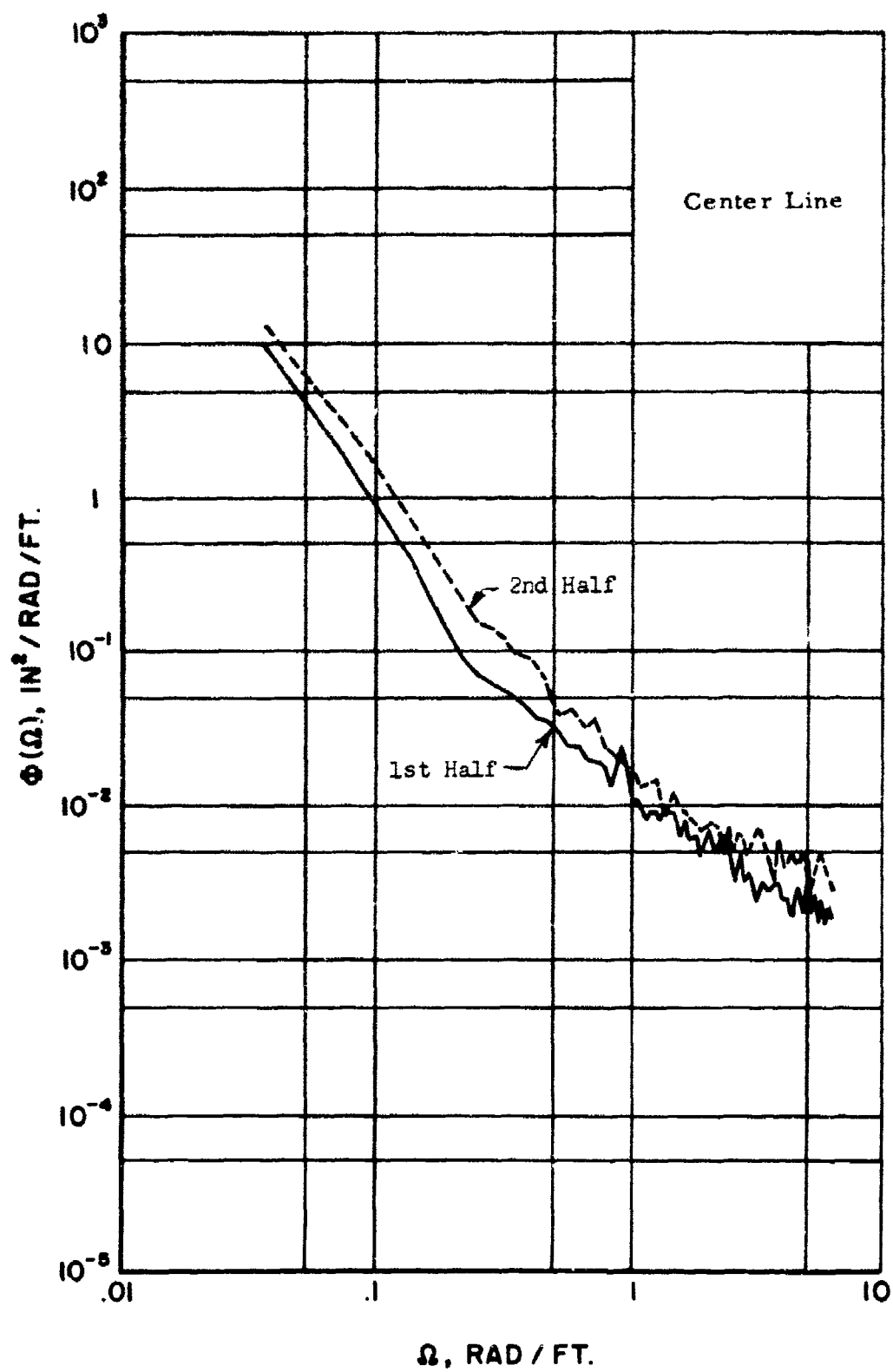


Fig. 11 Hughes Sod Field PSD Comparisons (First Half of the Runway Compared to the Second Half)

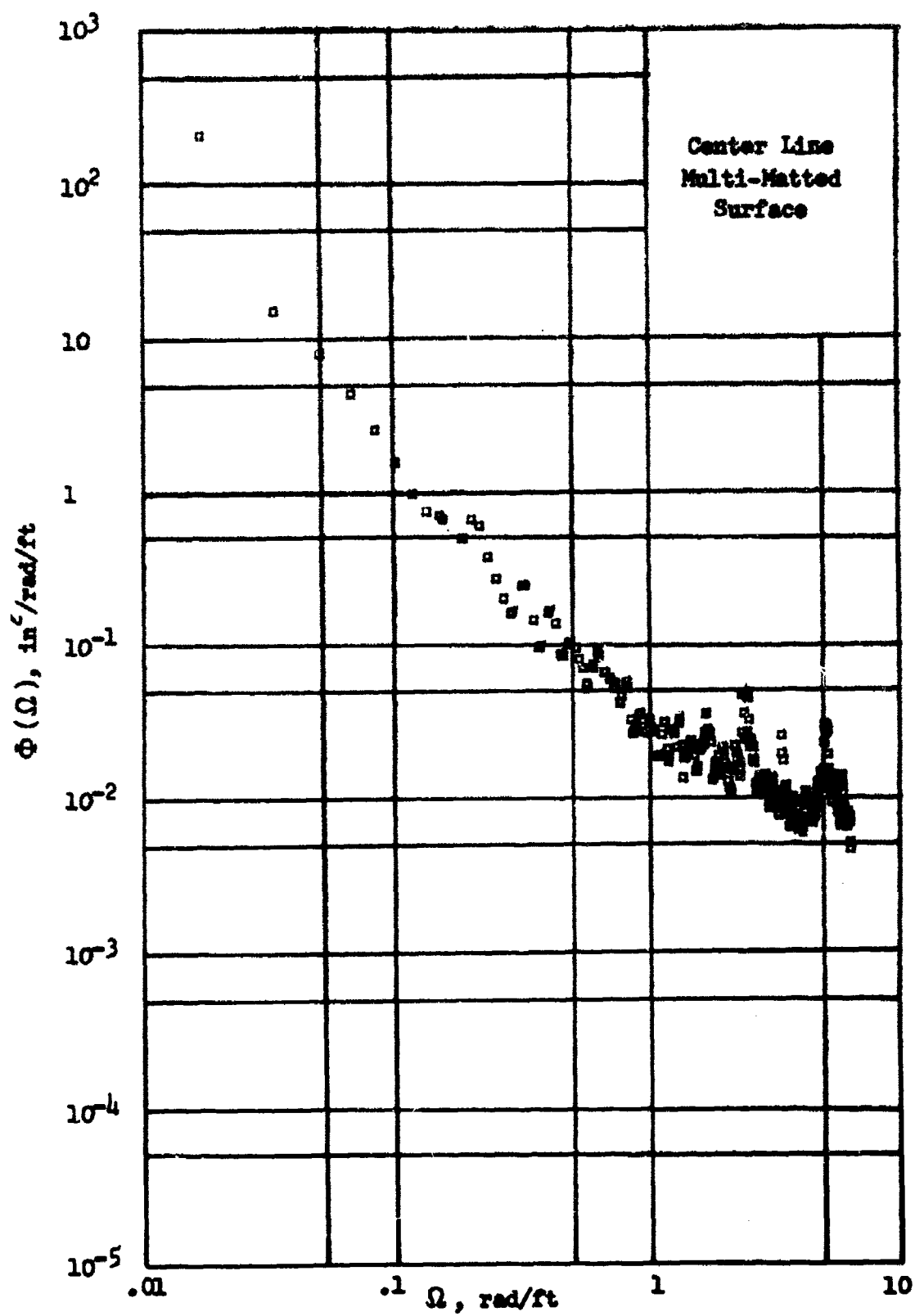


Fig. 12 Landing Surface Power Spectral Density, Runway 31, USMC Base, 29 Palms

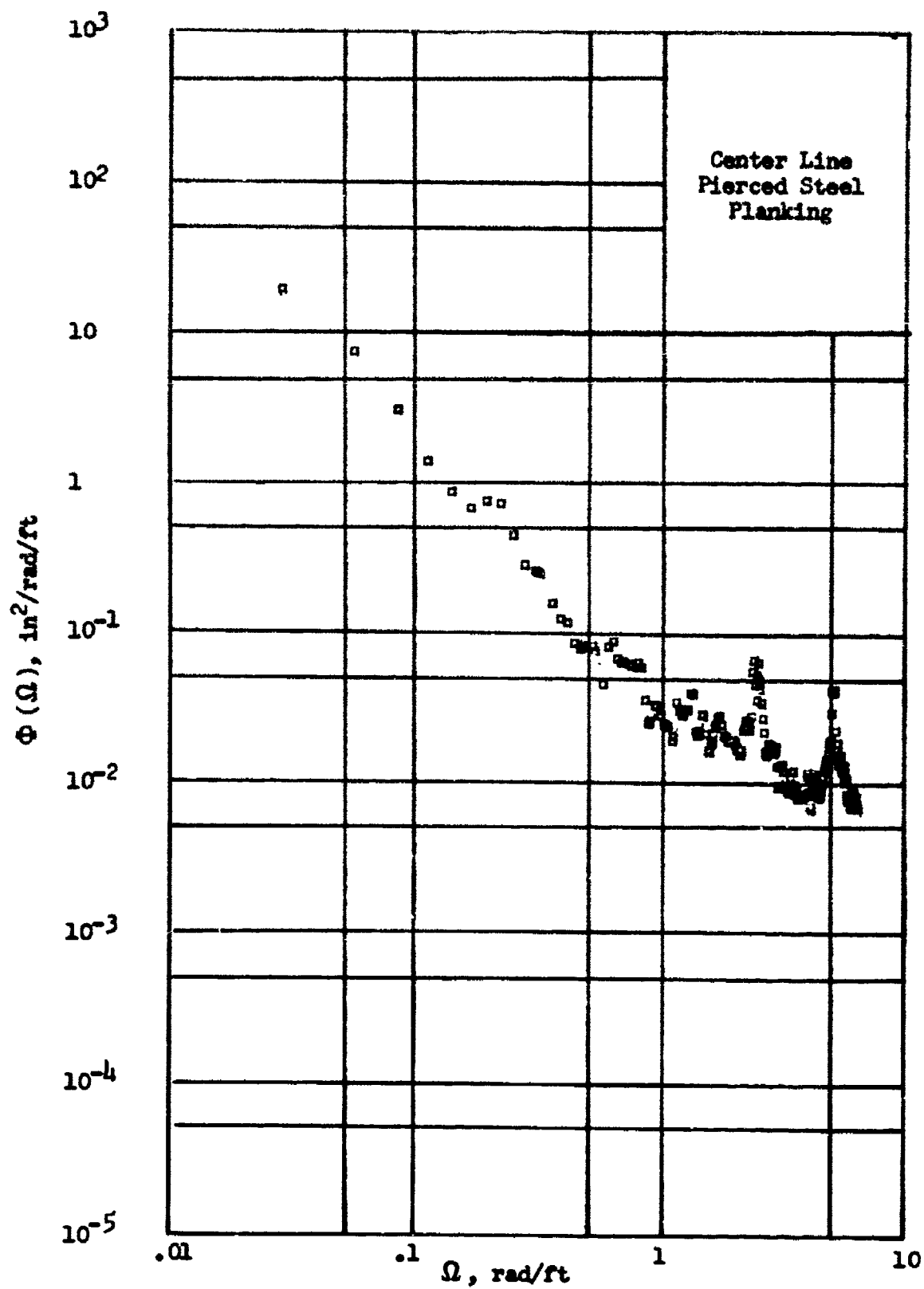


Fig.13 Landing Surface Power Spectral Density, Runway 31, USMC Base, 29 Palms

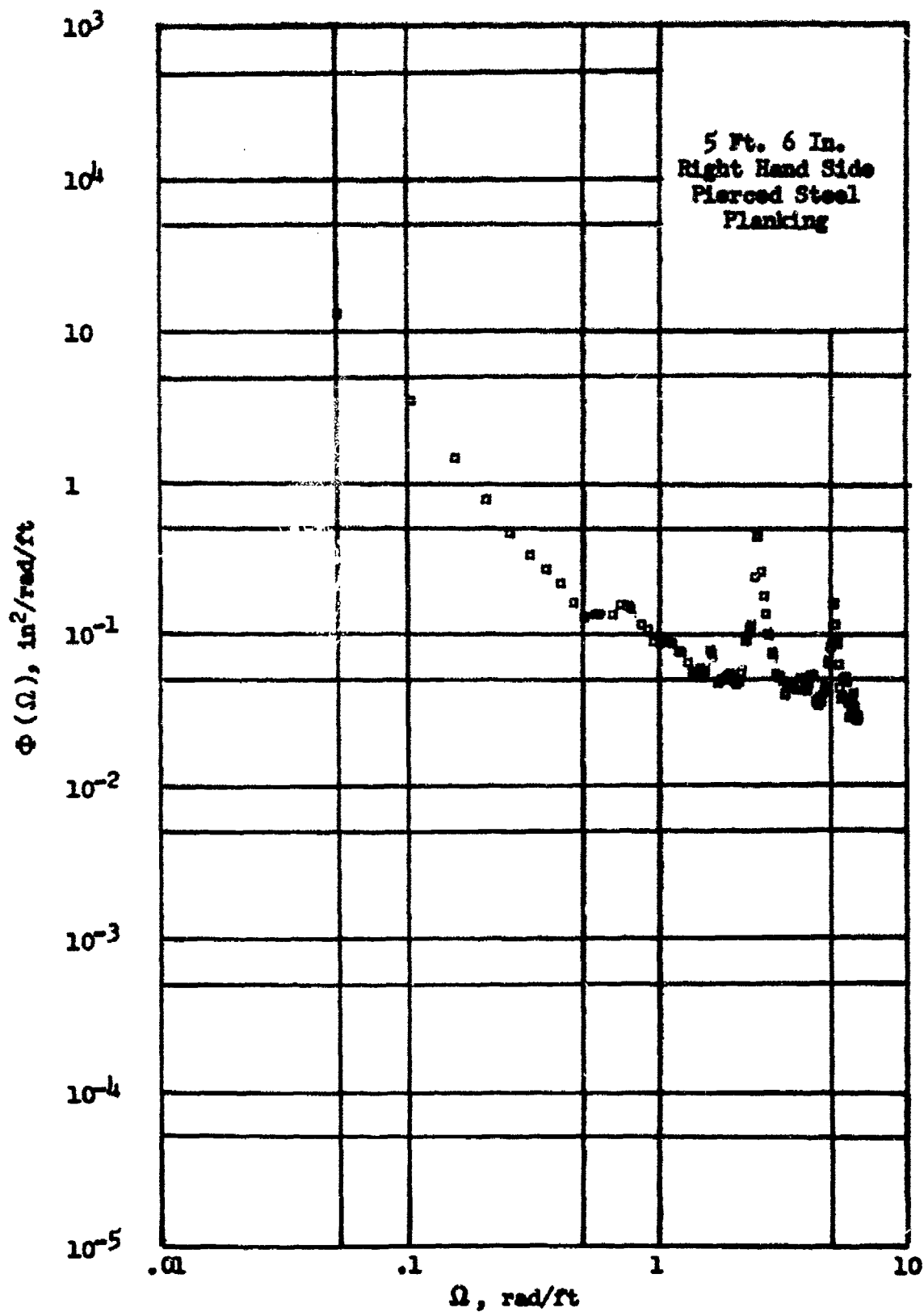


Fig. 14 Landing Surface Power Spectral Density, Runway 21, USMC Base, 29 Palms

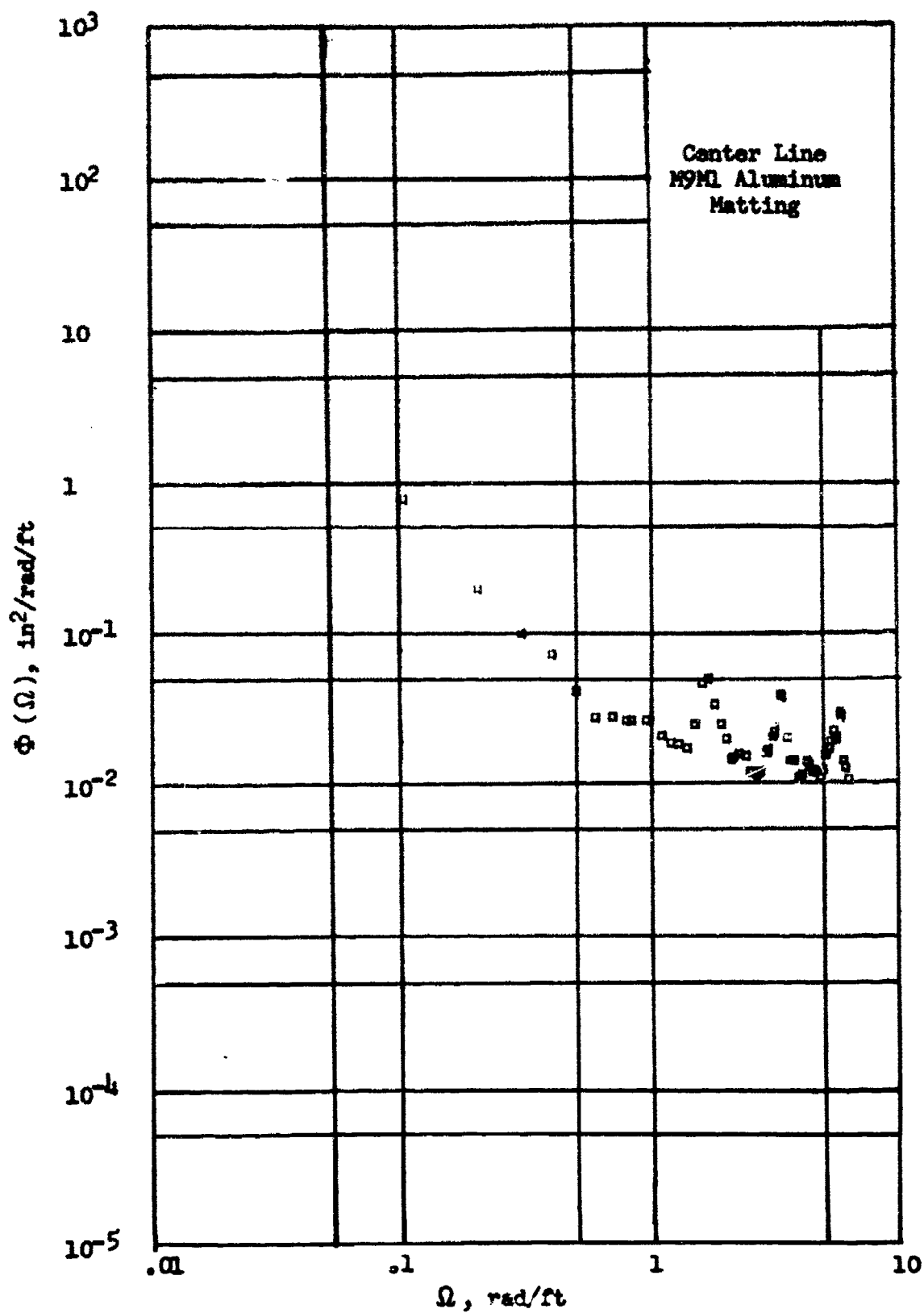
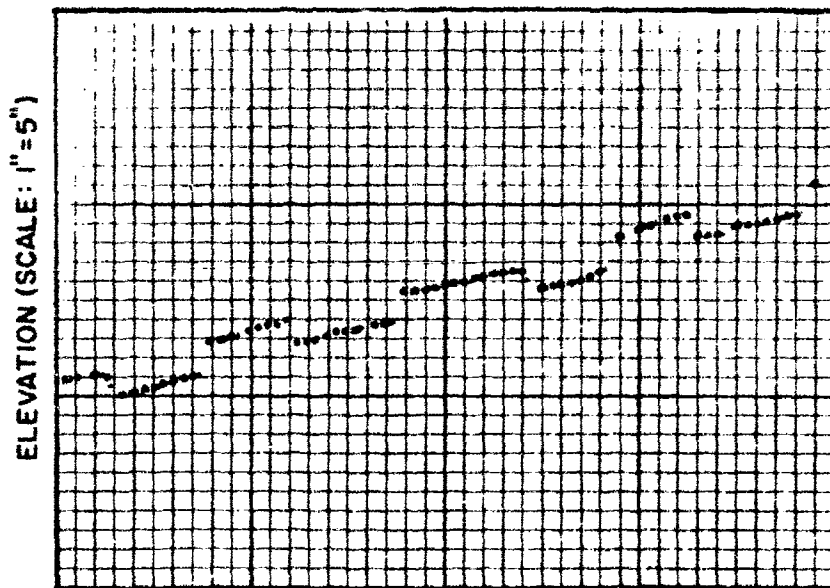


Fig. 15 Landing Surface Power Spectral Density, Runway 31, USMC Base, 29 Palms



RUNWAY DISTANCE (SCALE : 1" = 10')

Fig.16 Convair Aluminum Matting Profile

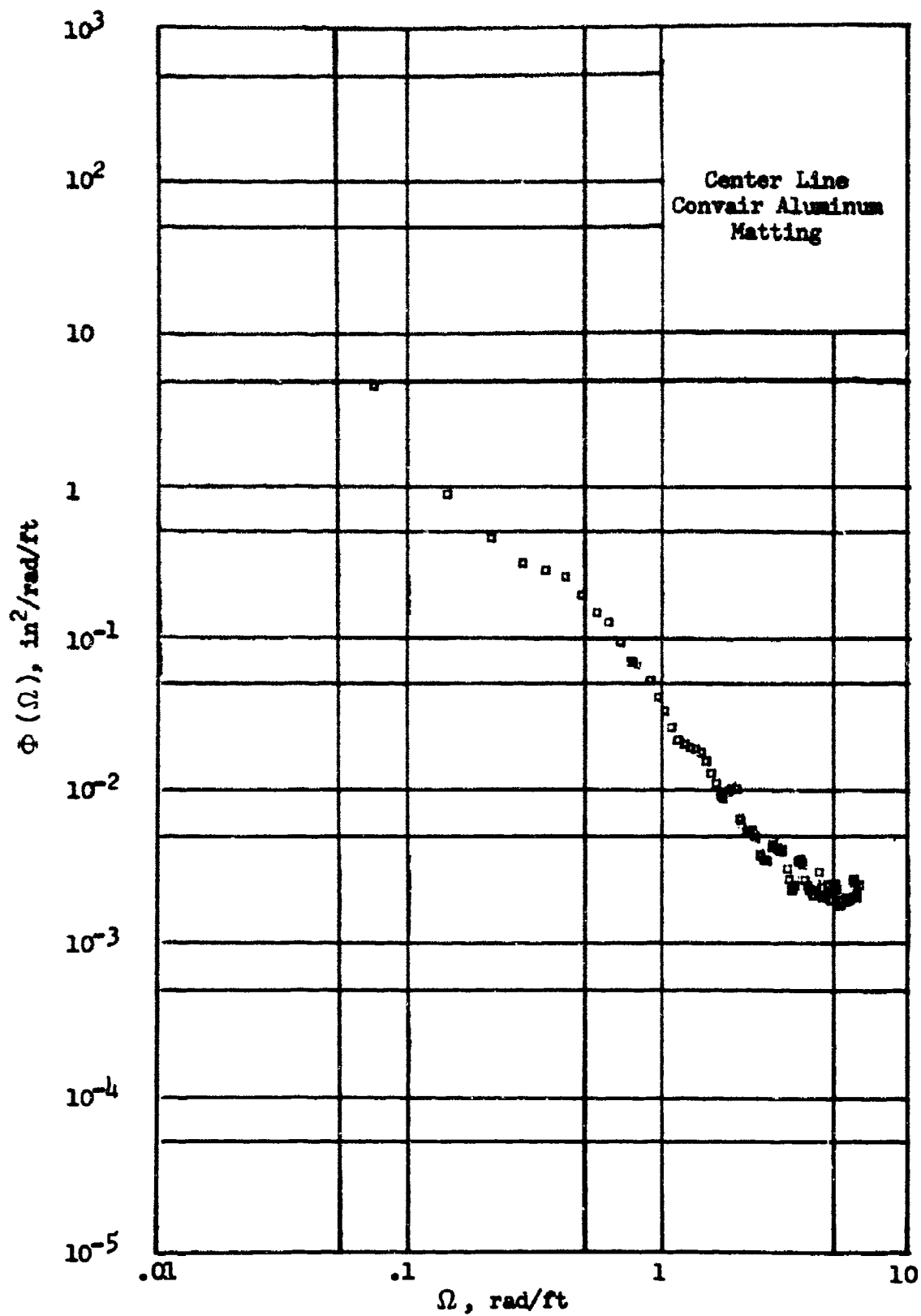


Fig.17 Landing Surface Power Spectral Density, Runway 31, USMC Base, 29 Palms

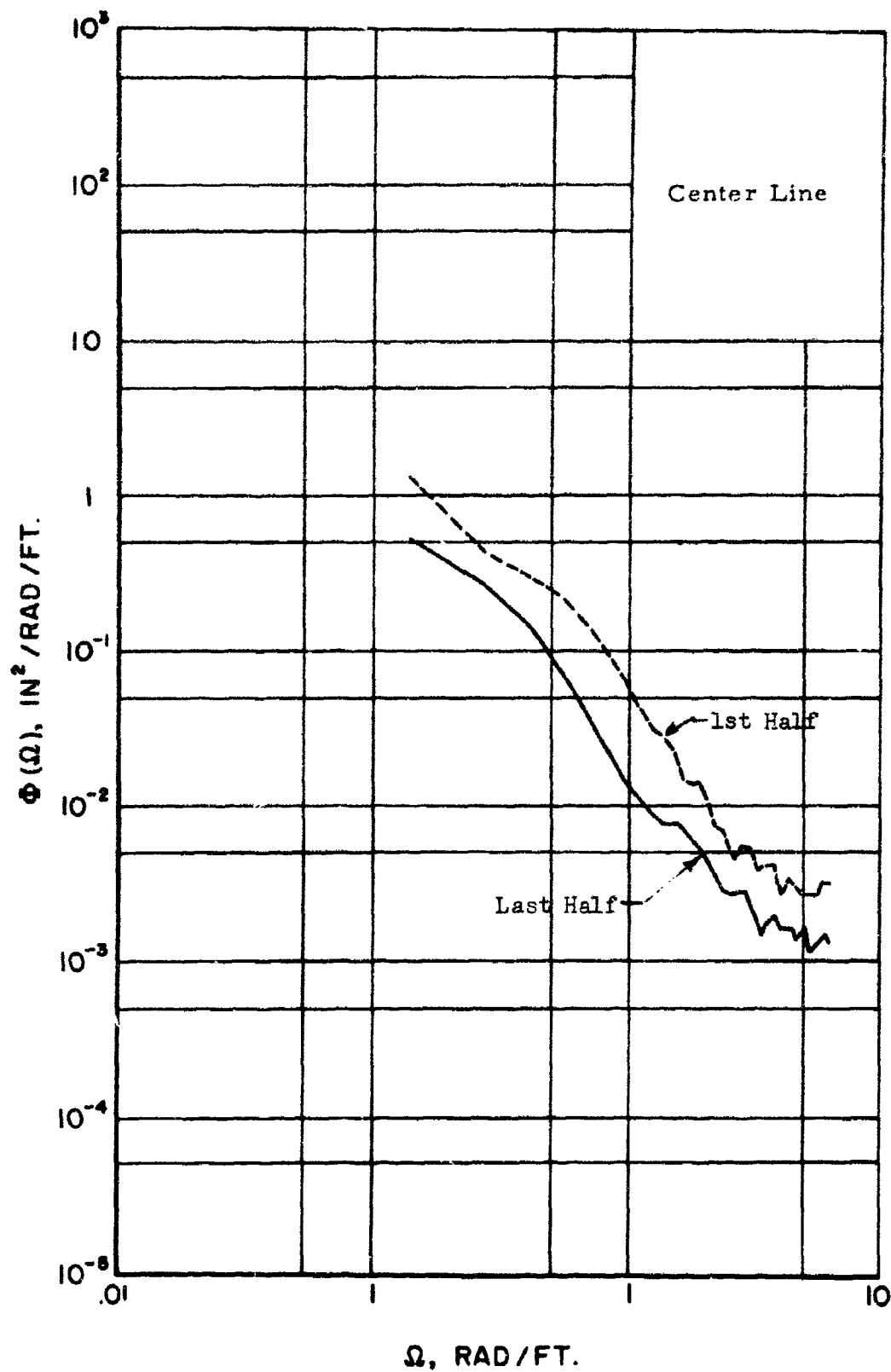


Fig. 18 Multi-Matted Runway PSD Comparisons (First Half of the Convair Matting Compared with the Last Half)

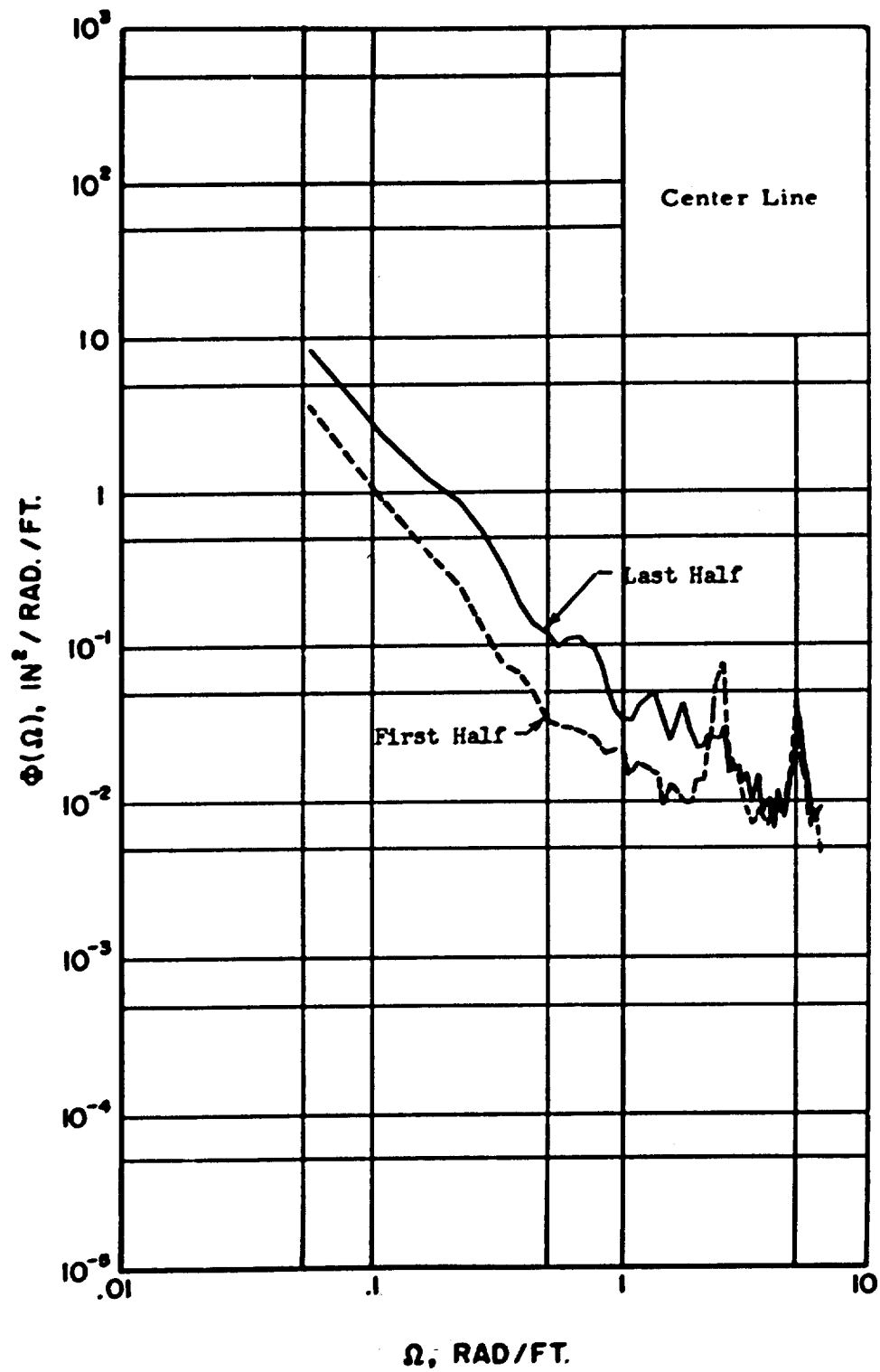


Fig. 19 Multi-Matted Runway PSD Comparisons (First Half of the Pierced Steel Planking Compared to the Last Half)

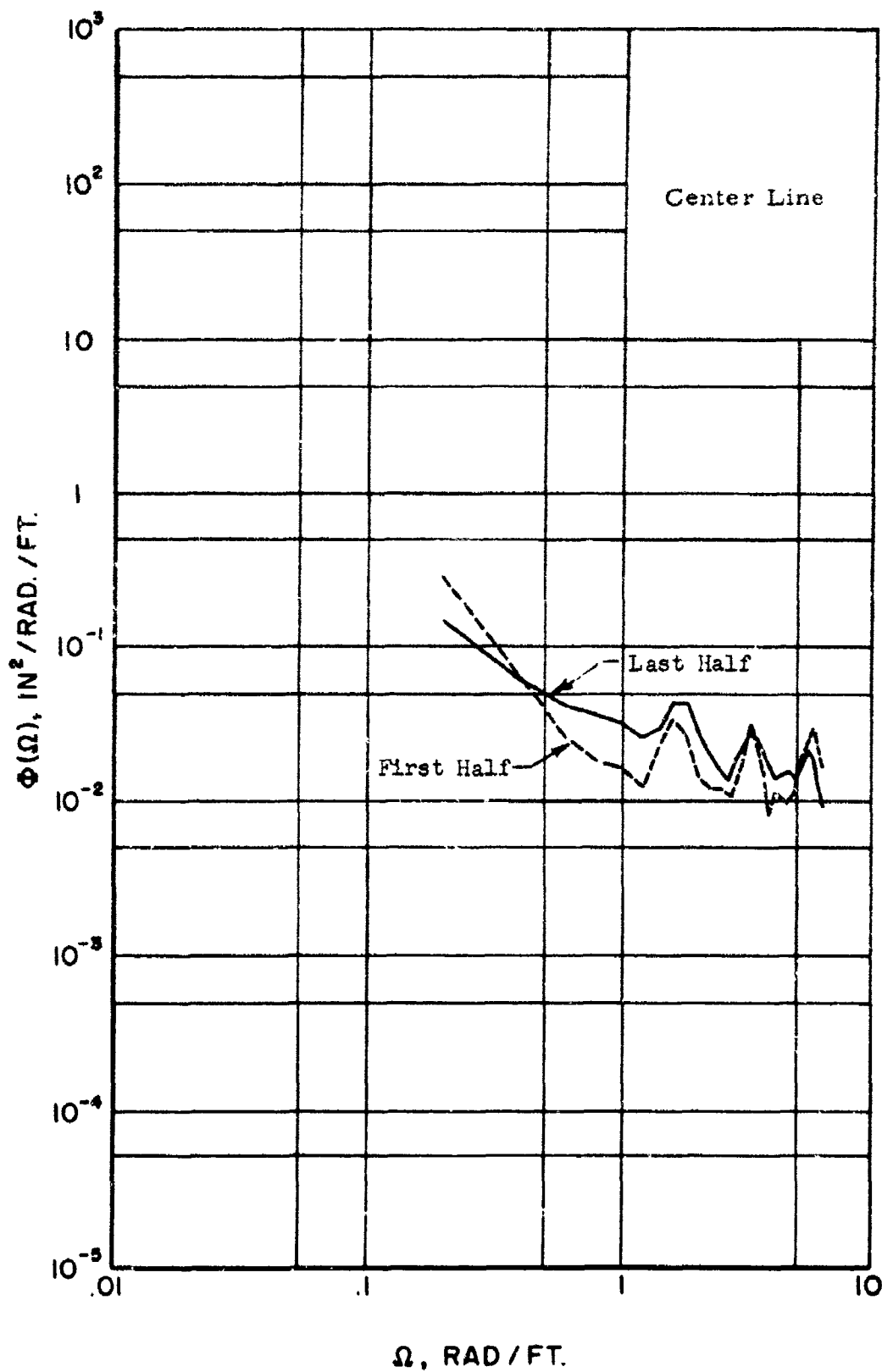


Fig. 20 Multi-Matted Runway PSD Comparisons (First Half of the M9M1 Aluminum Matting Compared to the Last Half)

FIG. 21 DISTRIBUTION OF MAXIMUM BUMP HEIGHT
(HUGHES SOD FIELD)

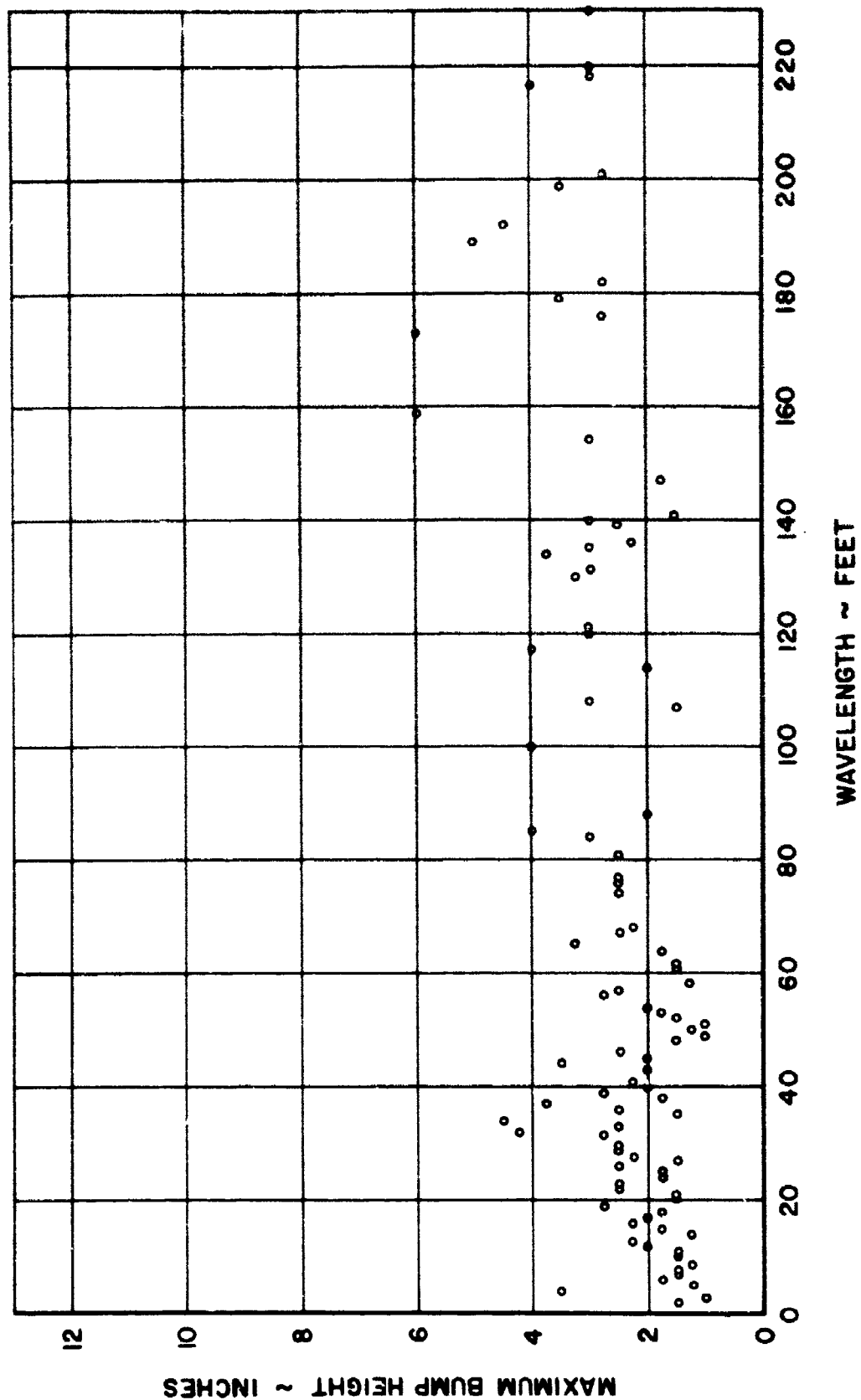
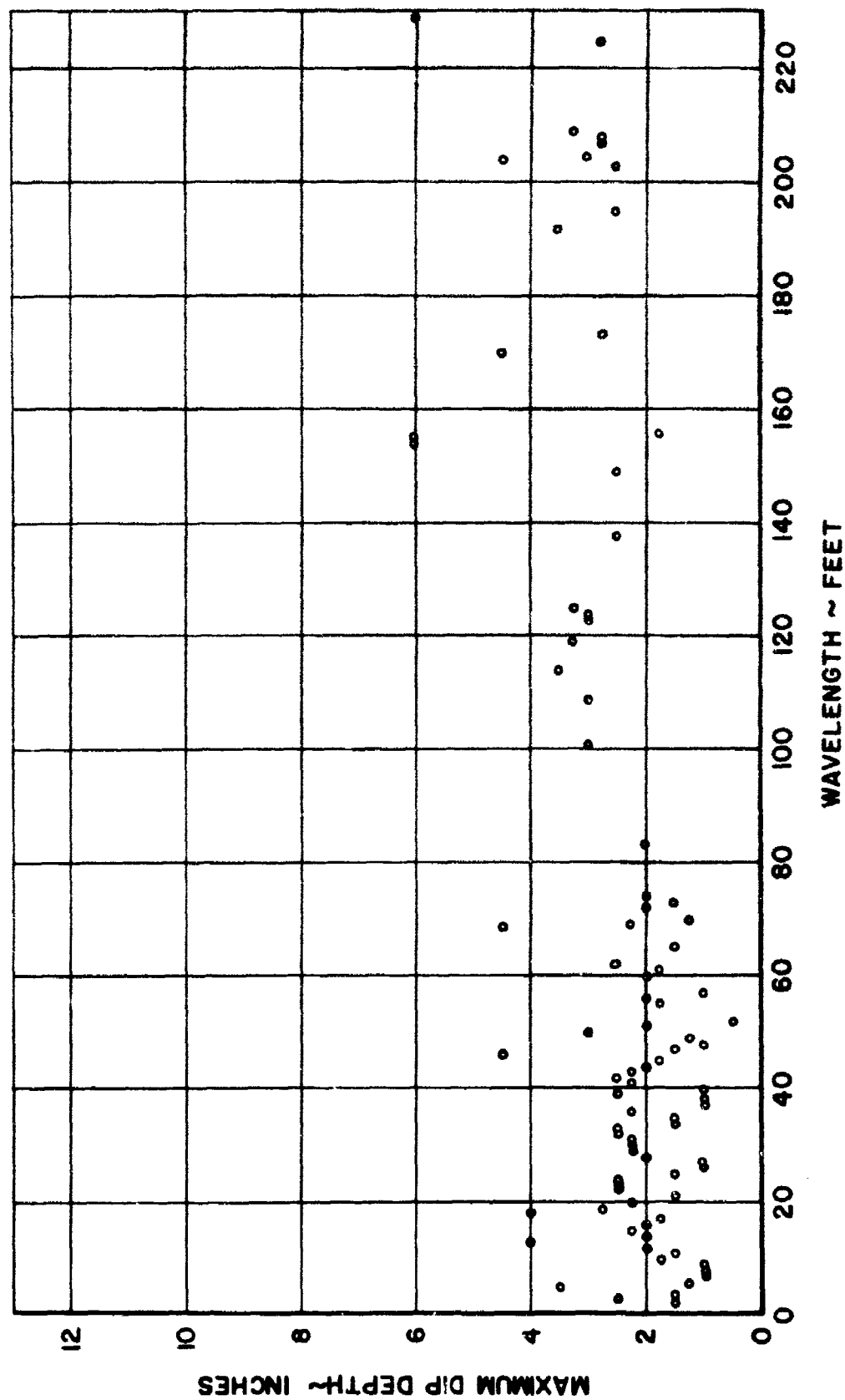


FIG. 22 DISTRIBUTION OF MAXIMUM DIP DEPTH
(HUGHES SOD FIELD)



**FIG. 23 DISTRIBUTION OF MAXIMUM BUMP HEIGHT
(MULTI-MATTED SURFACE)**

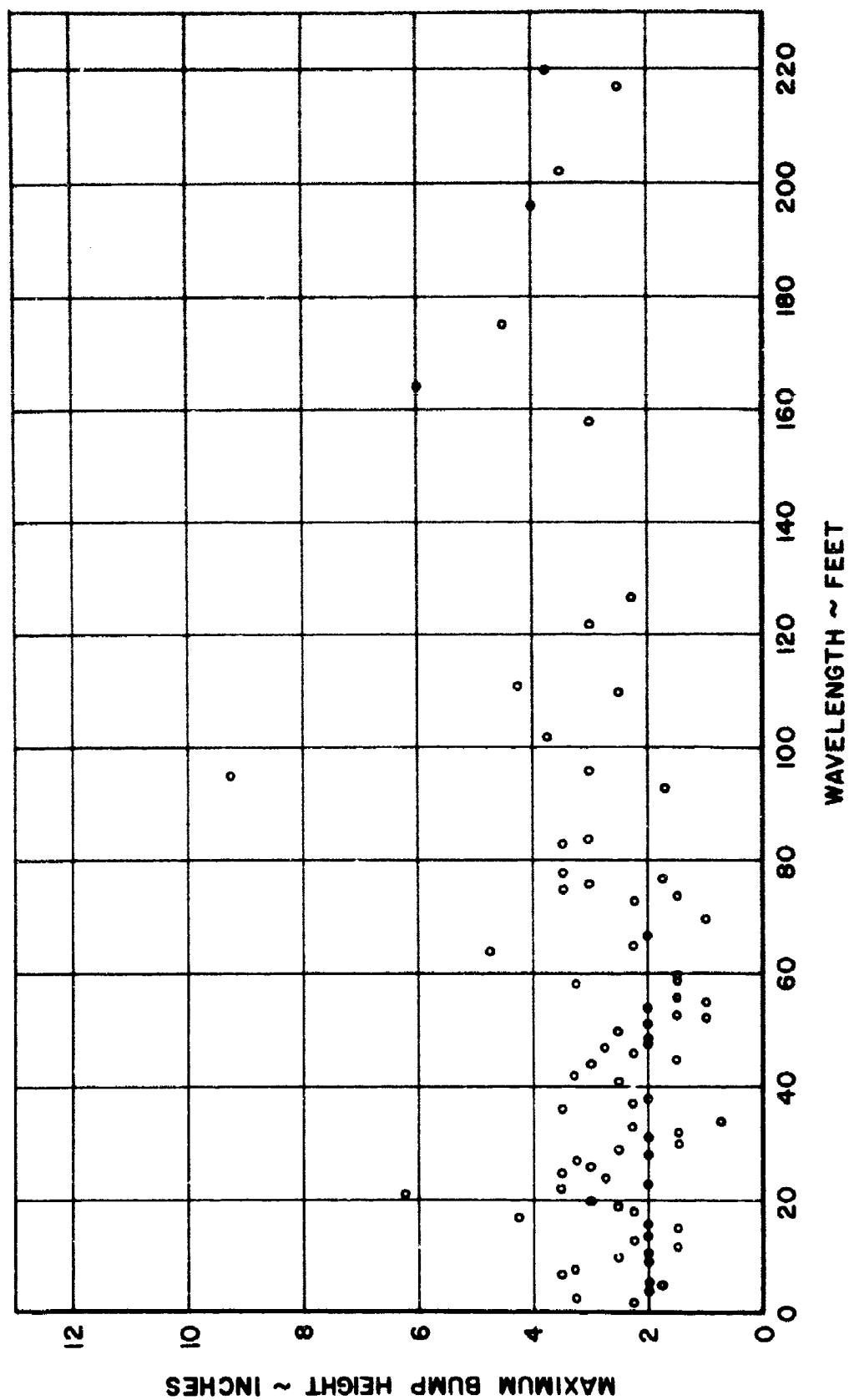


FIG. 24 DISTRIBUTION OF MAXIMUM DIP DEPTH
(MULTI - MATTED SURFACE)

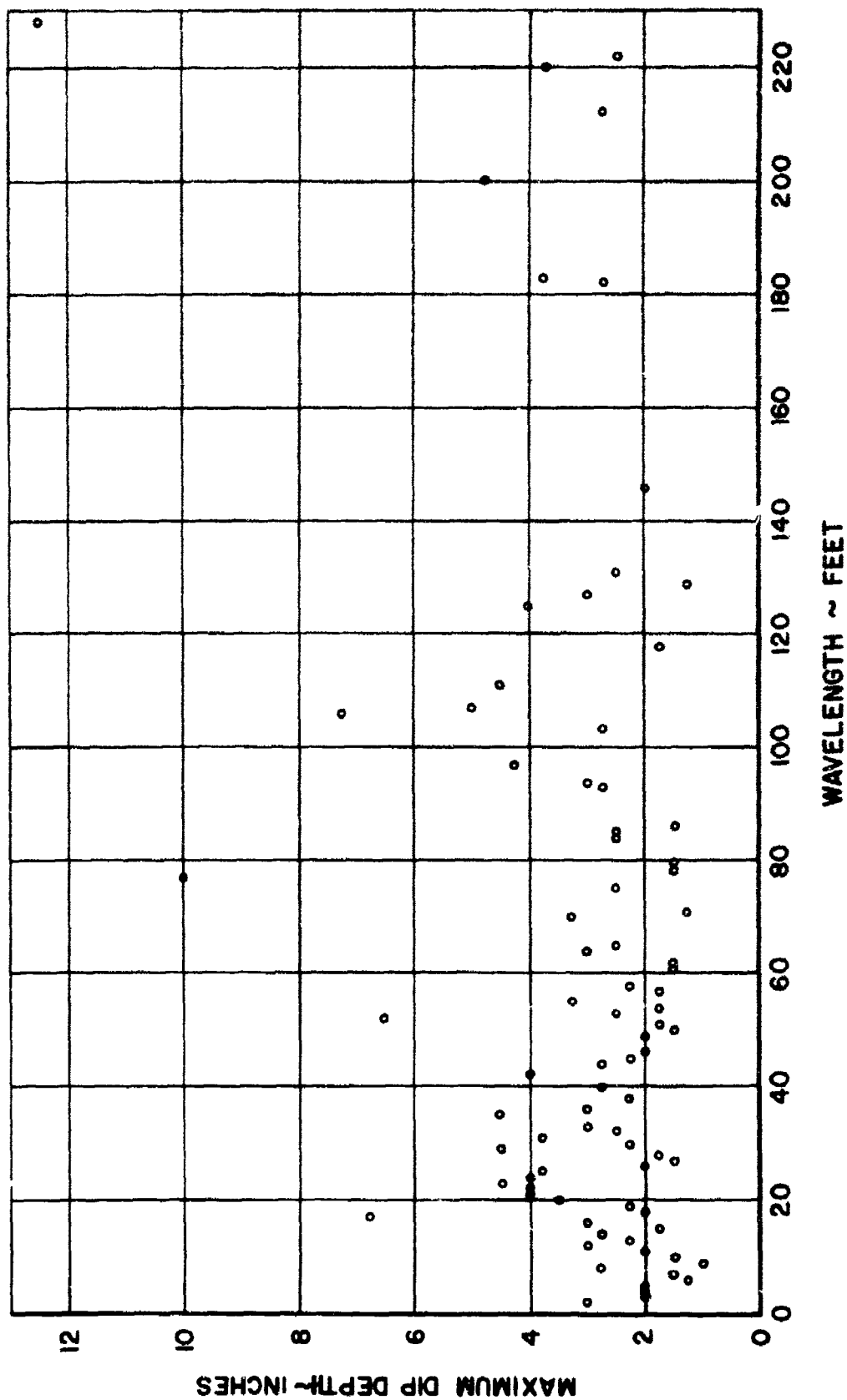


TABLE I

32

TABLE 1 (CONT'D)
DISTRIBUTION OF BUMPS BY HEIGHT AND WAVELENGTH
(HUGHES SOD FIELD)

λ	29	30	31	32	33	34	35	36	37	38	39	40	41	43	44	45	46	48	49	50	51	52	53	54	56	57	58
0.50					1			1																			
0.75	1	1		1			3	1													1						
1.00	3	4	1	2	2	2		3	3		1	3				1	1	1	1		2						
1.25	1					1				2	1					1	2					1		1			1
1.50	1	3		1	1		2		3		1					1		1				1	1				
1.75		1						1		2					1							1					
2.00		2										1	1	1									1				
2.25	1		1	1									1		1	1	1							1			
2.50	2	2			2			1									1									1	
2.75			1								2														1		
3.00				1																							
3.25											2																
3.50									1						1												
3.75															2												
4.00																											
4.25				1																							
4.50						1																					
5.00																											
6.00																											

TABLE 1 (CONT'D)

DISTRIBUTION OF BUMPS BY HEIGHT AND WAVELENGTH
(HUGHES SOD FIELD)

λ	141	147	154	159	173	176	179	182	189	192	199	201	217	218	220	230
0.50																
0.75																
1.00																
1.25																
1.50	1															
1.75		1														
2.00																
2.25																
2.50				2												
2.75						1	1	1			1					
3.00			1									1	1	1		
3.25																
3.50					1	1	1			1						
3.75																
4.00												1				
4.25																
4.50									1							
5.00																
6.00			1	1	1				1							

TABLE 2 (CONT'D)

DISTRIBUTION OF DIPS BY HEIGHT AND WAVELENGTH
(HUGHES SOD FIELD)

λ	29	30	31	32	33	34	35	36	37	38	39	40	41	42	43	44	45	46	47	48	49	50	51	52	55	56	57
0.50																											
0.75									1		1				1			1						1			
1.00	1	5	1	2		2	3	1	1	1	2	1			1	2	1	1	1								
1.25						2					2		1								1	1					1
1.50		1	1		1	1	1				1		3	2	3	1		1	1			2		1			
1.75	2			1																							
2.00		1			1								1	1		1	1					1					
2.25	1	1	2					2					2	2	1								1			1	
2.50				1	1						1			1													
2.75																											
3.00																											
3.25																						2					
3.50																											
3.75																											
4.00																											
4.50																		1									
6.00																											

TABLE 2 (CONT'D)
DISTRIBUTION OF DIPS BY HEIGHT AND WAVELENGTH
(HUGHES SOD FIELD)

[illegible]

TABLE 2 (CONT'D)

TABLE 2 (CONT'D)
DISTRIBUTION OF DIPS BY HEIGHT AND WAVELENGTH
(HUGHES SOD FIELD)

λ h	204	205	207	208	209	225	229	234	238	239	242
0.50											
0.75											
1.00											
1.25											
1.50											
1.75											
2.00											
2.25			1	1							
2.50											
2.75	1				1						
3.00	1							1	1		
3.25					1						
3.50								1			1
3.75											
4.00											
4.50	1										
6.00							1				

TABLE 3
DISTRIBUTION OF BUMPS BY HEIGHT AND WAVELENGTH
(MULTI-MATTED SURFACE)

λ h	2	3	4	5	6	7	8	9	10	11	12	13	14	15	16	17	18	19	20	21	22	23	24	25	26	27	28
0.50	139	78	39	18	6	3	1	1		1																	
0.75	18	38	21	15	12	10	3	4	1		3	2				2	1						1				
1.00	29	26	14	8	6	6	3	1	4	1	1	1	1													1	1
1.25	20	23	13	5	2													1				1	2	1			
1.50	14	15	8	6	6	1		1	1	1	2	1	1	3	1		2		1	1	1	1				1	
1.75	2	3		2		1		1	1	1					1	1			1	1		1	1			1	
2.00	2	1	1		1	1		1	1	1		1	1		1	1	1					2	1	2		1	
2.25	1											1															
2.50									2									1			1		1		1		
2.75																											
3.00																									1		
3.25								1																		1	
3.50						1																		1			
3.75																											
4.00																											
4.25																1											
4.50																											
4.75																											
5.00																											
5.25																				1							
5.50																									1		
5.75																											
6.00																											
6.25																											
6.50																											
6.75																											
7.00																											
7.25																											
7.50																											
7.75																											
8.00																											
8.25																											
8.50																											
8.75																											
9.00																											
9.25																											

TABLE 3 (CONT'D)
DISTRIBUTION OF BUMPS BY HEIGHT AND WAVELENGTH
(MULTI-MATTED SURFACE)

λ h	29	30	31	32	33	34	36	37	38	41	42	44	45	46	47	48	49	50	51	52	53	54	55	56	58	59	60
0.50																											
0.75		1				1																					
1.00					1					1										1							
1.25	1		1																				1				
1.50	2	1		1			1		1	1		2	1			1	1				1	1		1		1	1
1.75					1							1							2			1					
2.00			1				1		1	1		1			1	1	1										
2.25								1						1													
2.50	1									1								1									
2.75															1												
3.00												1															
3.25											1														1		
3.50							1																				
3.75																											
4.00																											
4.25																											
4.50																											
4.75																											
6.00																											
6.25																											
6.50																											
9.25																											

TABLE 3 (CONT'D)
DISTRIBUTION OF BUMPS BY HEIGHT AND WAVELENGTH
(MULTI-MATTED SURFACE)

λ	64	65	67	70	73	74	75	76	77	78	83	84	93	95	96	102	110	111	122	127	158	164	175	196	202	217	220	250
0.50																												
0.75																												
1.00				1																								
1.25																1												
1.50			1														1											
1.75									1																			
2.00			1																									
2.25		1			1			1												1								
2.50																	1									1		1
2.75																												
3.00								1				1			1				1									
3.25																												
3.50							1			1															1			
3.75																											1	
4.00																								1				
4.25																												
4.50																							1					
4.75	1																											
6.00																						1						
6.25																												
6.50																												
9.25																												

TABLE 4

DISTRIBUTION OF DIPS BY HEIGHT AND WAVELENGTH
(MULTI-MATTED SURFACE)

λ h	2	3	4	5	6	7	8	9	10	11	12	13	14	15	16	17	18	19	20	21	22	23	24	25	26	27	28
0.50	127	96	34	15	10	5	1																				
0.75	15	24	24	14	10	6	5	3	3	1	1	2	2	1		1			1	1							
1.00	19	25	15	7	4		2	1	1				1	1			1			2							
1.25	22	17	7	5	2	1	1				2									1							
1.50	12	11	2	4		1	1		1		1	1	1		1	1	1		1			1	1			1	
1.75		3	2				1					1	1	3		1						1					2
2.00		1	2							2			2				1					1			1	2	
2.25	1		2									1			1			1									
2.50													1						1								
2.75							1						1														
3.00	2										1				1												
3.25																											
3.50																			1		1						
3.75																								1			
4.00																				1	1		1				
4.25																				1	1						
4.50																						1					
4.75																											
5.00																											
6.50																											
6.75																											
7.25																1											
10.00																											
12.50																											

TABLE 4 (CONT'D)
DISTRIBUTION OF DIPS BY HEIGHT AND WAVELENGTH
(MULTI-MATTED SURFACE)

λ h	29	30	31	32	33	35	36	38	40	42	44	45	46	49	50	51	52	53	54	55	57	58	61	62	64	65	70
0.50																											
0.75																											
1.00						1	1													1							
1.25																											
1.50		2	1		1	1		1	1		1	2	1		1		2					1	1				
1.75		1				1										1			1		1						
2.00		1	1				1		1				1	1						1							
2.25		1						1				1										1					
2.50				2	1													1								1	
2.75	1		1						2	1							1										
3.00						1																			1		1
3.25																				1							
3.50																											
3.75			1																								
4.00	1									1																	
4.25																											
4.50	1					1																					
4.75																											
5.00																											
6.50																	1										
6.75																											
7.25																											
10.00																											
12.50																											

TABLE 4 (CONT'D)
DISTRIBUTION OF DIPS BY HEIGHT AND WAVELENGTH
(MULTI-MATTED SURFACE)

λ	71	75	77	78	80	84	85	86	93	94	97	103	106	107	111	118	125	127	129	131	146	182	183	200	212	220	222	228
0.50																												
0.75																												
1.00																												
1.25	1																											
1.50			1	1				1											1									
1.75			1													1												
2.00																					1							
2.25																												
2.50		1				1	1													2								
2.75									1			1										1					1	
3.00										1								1										
3.25																												
3.50																												
3.75																												
4.00																												
4.25											2				1													
4.50																												
4.75																												
5.00																												
6.50																												
6.75																												
7.25																												
10.00			1										1															
12.50																												

SECTION VI

REFERENCES

1. Automatic Runway Profile Measuring Instrumentation and Runway Properties, Part I - Equipment, WADD-TR-60-470, Part I
2. Automatic Runway Profile Measuring Instrumentation and Runway Properties, Part III - Base Surveys, WADD TR 60-470, Part III
3. Design Criteria for Ground-Induced Dynamic Loads, RTD-TDR-63-4139, Volumes I and II